CORE
Metadata, citation and similar papers at core.ac.uk
Provided by NASA Technical Reports Server

NASA CONTRACTOR REPORT

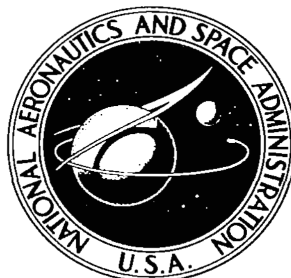

NASA CR-40

LOAN COPY: RETURN TO
AFWL (WLIL-2)
KIRTLAND AFB, N MEX

NASA CR-404

EFFECTS OF LOW ENERGY PROTONS AND HIGH ENERGY ELECTRONS ON SILICON

by J. R. Carter and R. G. Downing

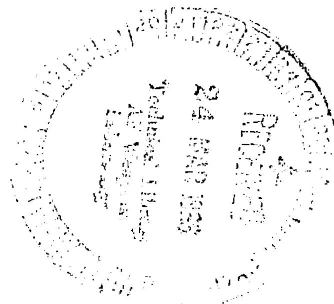

Prepared under Contract No. NAS 5-3805 *by*
TRW SPACE TECHNOLOGY LABORATORIES
Redondo Beach, Calif.
for Goddard Space Flight Center

NATIONAL AERONAUTICS AND SPACE ADMINISTRATION • WASHINGTON, D. C. • MARCH 1966

TECH LIBRARY KAFB, NM

0099539

NASA CR-404

EFFECTS OF LOW ENERGY PROTONS AND HIGH ENERGY ELECTRONS ON SILICON

By J. R. Carter and R. G. Downing

Distribution of this report is provided in the interest of information exchange. Responsibility for the contents resides in the author or organization that prepared it.

Prepared under Contract No. NAS 5-3805 by
TRW SPACE TECHNOLOGY LABORATORIES
Redondo Beach, Calif.

for Goddard Space Flight Center

NATIONAL AERONAUTICS AND SPACE ADMINISTRATION

For sale by the Clearinghouse for Federal Scientific and Technical Information
Springfield, Virginia 22151 – Price $0.90

ACKNOWLEDGMENTS

This report covers work performed under Contract NAS5-3805 during the period from 5 May 1964 to 5 May 1965. We would like to acknowledge the helpful guidance of and discussions with Mr. Milton Schach and Dr. Paul Fang of NASA Goddard Space Flight Center during conduct of this program. We would also like to acknowledge the cooperation and assistance of the personnel at the electron accelerator facilities of General Atomic and Shell Development Co. during the course of the experiments and the many semiconductor organizations who provided the material upon which these studies were based.

ABSTRACT

Using Hall effects measurements, the electron energy dependence of the defect introduction ratesof the E_c - 0.17 ev, E_c - 0.4 ev, and E_v + 0.3 ev levels has been determined. The two levels at E_c - 0.17 ev and E_c - 0.4 ev are found to be relatively insensitive to incident electron energy as predicted by simple displacement theory. The defect introduction rate for the E_v + 0.3 ev level is found to increase rapidly with increasing electron energy. It is also observed that the energy dependence of the E_v + 0.3 ev level appears to be a function of material resistivity in that the dependence becomes steeper at lower resistivities. At resistivities of the order of 15 ohm-cm the energy dependence of the defect introduction rate of the E_v + 0.3 ev level is identical to the observed energy dependence of the degradation of minority carrier lifetime in 10 ohm-cm n on p silicon solar cells. Empirically it is observed that this energy dependence appears to be proportional to the second power of the simple displacement theory, suggesting that these defects may be associated with a divacancy or other double displacement type defect.

Under low energy proton bombardment in the energy range from 0.2 Mev to 1.9 Mev the degradation rates of open circuit voltage, short circuit current and maximum power are much greater than normally observed for penetrating radiation. The maximum sensitivity of absolute power degradation of silicon solar cells appears to lie at or slightly above 2 Mev with decreasing sensitivity evidenced at energies below 2 Mev and above 6 Mev. In addition, considerable room temperature annealing in periods of times of the order of days is observed for low energy proton damaged cells in contrast to that observed for cells damaged with more penetrating radiation.

One Mev electron irradiation of 1 ohm-cm and 10-ohm-cm boron doped and aluminum doped n on p silicon solar cells indicate that the differences in radiation sensitivity as measured by K values cannot be attributed to the dopant material. It was also observed that differences in K values were greater between specimen lots than between the differently doped specimens of equal resistivities, suggesting that fabrication techniques or differences in bulk material trace impurity content may be responsible for the observed small differences in radiation sensitivity.

TABLE OF CONTENTS

		Page
I.	INTRODUCTION.	1
II.	RADIATION INDUCED ENERGY LEVELS IN SILICON.	2
	Experimental Techniques	3
	Results	4
	Discussion.	11
	Conclusions	24
III.	LOW ENERGY PROTON DEGRADATION IN SILICON SOLAR CELLS. .	25
	Experimental Techniques	25
	Results	27
	Conclusions	34
IV.	EFFECT OF IMPURITIES ON RADIATION DAMAGE IN SILICON . .	37
	Experimental Techniques	37
	Results	39
	Conclusions	46
V.	SUMMARY	47
REFERENCES		49

LIST OF ILLUSTRATIONS

Figure		Page
1	Temperature Variation of Reciprocal Hall Coefficient for 100 Ω -cm, n-type Silicon before and after Electron Irradiation (1.0 Mev).	5
2	Temperature Variation of Reciprocal Hall Coefficient for 100 Ω -cm, n-type Silicon before and after Electron Irradiation (2.0 Mev).	6
3	Temperature Variation of Reciprocal Hall Coefficient for 100 Ω -cm, n-type Silicon before and after Electron Irradiation (3.0 Mev).	7
4	Temperature Variation of Reciprocal Hall Coefficient for 100 Ω -cm, n-type Silicon before and after Electron Irradiation (4.7 Mev).	8
5	Temperature Variation of Reciprocal Hall Coefficient for 100 Ω -cm, n-type Silicon before and after Electron Irradiation (15 Mev)	9
6	Temperature Variation of Reciprocal Hall Coefficient for 100 Ω -cm, n-type Silicon before and after Electron Irradiation (35 Mev)	10
7	Introduction Rate of the E_c - 0.4 ev and E_c - 0.17 ev Levels in n-type Silicon for Electrons of Various Energies	14
8	Temperature Variation of Reciprocal Hall Coefficient for 15 ohm-cm p-type Silicon Before and After Electron Irradiation (0.7 Mev).	15
9	Temperature Variation of Reciprocal Hall Coefficient for 15 ohm-cm p-type Silicon Before and After Electron Irradiation (1.0 Mev).	16
10	Temperature Variation of Reciprocal Hall Coefficient for 15 ohm-cm p-type Silicon Before and After Electron Irradiation (3.0 Mev).	17
11	Temperature Variation of Reciprocal Hall Coefficient for 15 ohm-cm p-type Silicon Before and After Electron Irradiation (11.5 Mev)	18

LIST OF ILLUSTRATIONS (Con't)

Figure		Page
12	Introduction Rate of the E_v + 0.3 ev Level in Silicon for Electrons of Various Energies.	19
13	Electron Energy Dependence of Φ^{-1} Values for n on p Silicon Solar Cells.	23
14	Silicon Solar Cell Short Circuit Current Degradation Under Low Energy Proton Irradiation.	29
15	Comparison of Sun Simulator Data with 2800°K Tungsten Data	31
16	Silicon Solar Cell Open Circuit Voltage Degradation Under Low Energy Proton Irradiation.	33
17	Degradation of Maximum Power Output for Silicon Solar Cells Under Low Energy Proton Irradiation.	35
18	Short Circuit Current Degradation of 1 ohm-cm Silicon Solar Cells Under Electron Irradiation	41
19	Minority Carrier Diffusion Length Degradation of 1 ohm-cm Silicon Under Electron Irradiation	42
20	Short Circuit Current Degradation of 10 ohm-cm Silicon Solar Cells Under Electron Irradiation	44
21	Minority Carrier Diffusion Length Degradation of 10 ohm-cm Silicon Under Electron Irradiation.	45

TABLE I	Summary of Data.	12-13
TABLE II	K Values for Aluminum and Boron Doped Silicon.	43

I. INTRODUCTION

The efforts described in this report range from the acquisition of important design data on contemporary silicon solar cells under low energy proton bombardment to basic research on the fundamentals of defect formation in silicon by electron and proton radiation of the type found in space. Although the complete understanding and solution of problems concerning the use of semiconductor devices in space is beyond the scope of any single program, it is felt that the work presented here, coupled with similar efforts by others in the field, will lead to further stimulation, better understanding, and more efficient solutions to these problems.

The work reported here encompasses three general areas of investigation. In Section II the electron energy dependence of the defect introduction rate for several energy levels is presented for both p-type and n-type silicon. In Section III data is presented on the effect of low energy proton bombardment of silicon solar cells. In Section IV aluminum doped p-type silicon and boron doped p-type silicon of resistivities of 1 and 10 ohm-cm are investigated in terms of their radiation sensitivity to 1 Mev electrons.

II. RADIATION INDUCED ENERGY LEVELS IN SILICON

Despite considerable study of electron damage in silicon, the nature of the defects controlling degradation in silicon devices is not clear. Wertheim's work indicated that electrons of 0.7 Mev introduce recombination centers in n-type silicon at 0.27 ev above the valence band and in p-type silicon at 0.17 ev below the conduction band[1,2]. Galkin, et al,[3] have reported that 1.0 Mev electrons produce recombination centers in n-type silicon at 0.16 ev below the conduction band. Baicker has reported evidence that the dopant used in n-type silicon may influence the recombination center produced by electron damage[4]. In p-type electron irradiated silicon, he has suggested that a recombination center at 0.18 ev above the valence band controls recombination. In addition, it has been shown that the annealing characteristics of recombination centers in both n- and p-type silicon irradiated with 0.7 Mev electrons are identical to those of the silicon A center (E_c - 0.17 ev)[5,6]. Work done at STL has indicated that the E_c - 0.17 ev level controls recombination in p-type silicon irradiated with 1.0 Mev electrons[7]. The nature of the radiation defects controlling recombination in electron irradiated silicon is still very much in doubt because of the conflicting conclusions reported.

All of the work reported in the above references involved some direct measurements of minority carrier lifetime which were analyzed in terms of Hall-Shockley-Read statistics. This direct approach is subject to many experimental difficulties because of the low lifetimes involved in irradiated silicon. The work reported here involves an indirect approach to the problem of identifying the irradiation produced recombination centers. The introduction rates of various defect levels were determined for electrons of various energies. These data are compared with the energy variation of degradation studies on solar cells. The critical fluxes and damage constants have been determined for n on p and p on n solar cells irradiated with electrons of various energies[7]. In the simplest case, the energy dependence of the recombination center intro-

duction rate should be similar to the energy dependence of these critical fluxes and damage constants. Such agreement is not conclusive evidence for identification of recombination centers, but it can support or question previous conclusions.

The introduction rates of the defect levels were measured by the Hall coefficient technique. These techniques have been used in several investigations for detecting defect energy levels[1,2,3,8]. Previous work was concentrated on lower energies, whereas, this work included electrons to 35 Mev. In addition to the Hall measurements, considerable study of these defects by electron spin resonance has been reported[6,9,10,11]. Several defects have been characterized through this work. They are: an acceptor level at E_c - 0.17 ev (Si-A center), an acceptor level at E_c - 0.4 ev (Si-E center), a second acceptor level at E_c - 0.4 ev (Si-C center), and a donor level at E_v + 0.3 ev (Si-J center). Only one level at 0.4 ev has been reported by Hall measurements; however, the existence of two has been suggested by annealing studies[12].

A. Experimental Techniques

The irradiations reported were done at several facilities. The STL Van de Graaff was used for all electrons of 1 Mev and lower. The Shell Development Corporation Van de Graaff was used in the 1 to 3 Mev range. The General Atomic Linear accelerator was used for 4 to 35 Mev irradiations. All irradiations were done at room temperature and care was taken to avoid heating of the samples by the electron beam. Measurement of beam current, electron flux and Hall coefficient was instrumented as described previously[7,13]. The silicon used in this work was grown by the crucible method by Futurecraft Corporation. Dislocation density was below 100 per sq. cm. The principal dopants were phosphorus for n-type and boron for p-type. Resistivities varied from 1 to 150 ohm-cm.

The Hall coefficient of each sample was determined as a

function of temperature before and after irradiation. The Hall coefficient can be related to the majority carrier concentration by the following equation:

$$n = \frac{r}{Re} \qquad (1)$$

where n = concentration of majority carriers

R = Hall coefficient

e = electronic charge

r = Hall factor

The Hall factor was determined from Hall mobility and published drift mobilities[14]. The detection and determination of energy levels is covered by Wertheim[2] and Hill[8]. The defect introduction rate was determined as follows:

$$\eta = \frac{\left(\frac{1}{R_o} - \frac{1}{R}\right) \frac{r}{e}}{\Phi} \text{ (defects/electron-cm)} \qquad (2)$$

where R_o = Hall coefficient before irradiation

R = Hall coefficient after irradiation

Φ = Electron flux, e/cm^2

B. Results

The Hall data are analyzed in plots of reciprocal Hall coefficient versus reciprocal temperature. This plot can be easily interpreted since majority carrier concentration is very closely related to the reciprocal Hall coefficient and changes in carrier concentration are reflected by changes in Hall coefficient. Examples of this are shown in Figures 1 through 6. Figure 1 is typical of the response of n-type silicon to lower energy electrons. The data show evidence of one acceptor level at E_c - 0.17 ev. The E_c - 0.4 ev level is introduced at very low rates at 1 Mev and below. When electrons of much higher energy interact with n-type silicon, the E_c - 0.4 ev level is introduced in much higher rates. This effect is shown in Figures 4 through 6. The appearance of the E_c - 0.4 ev level is shown by the large decrease in carrier concentration

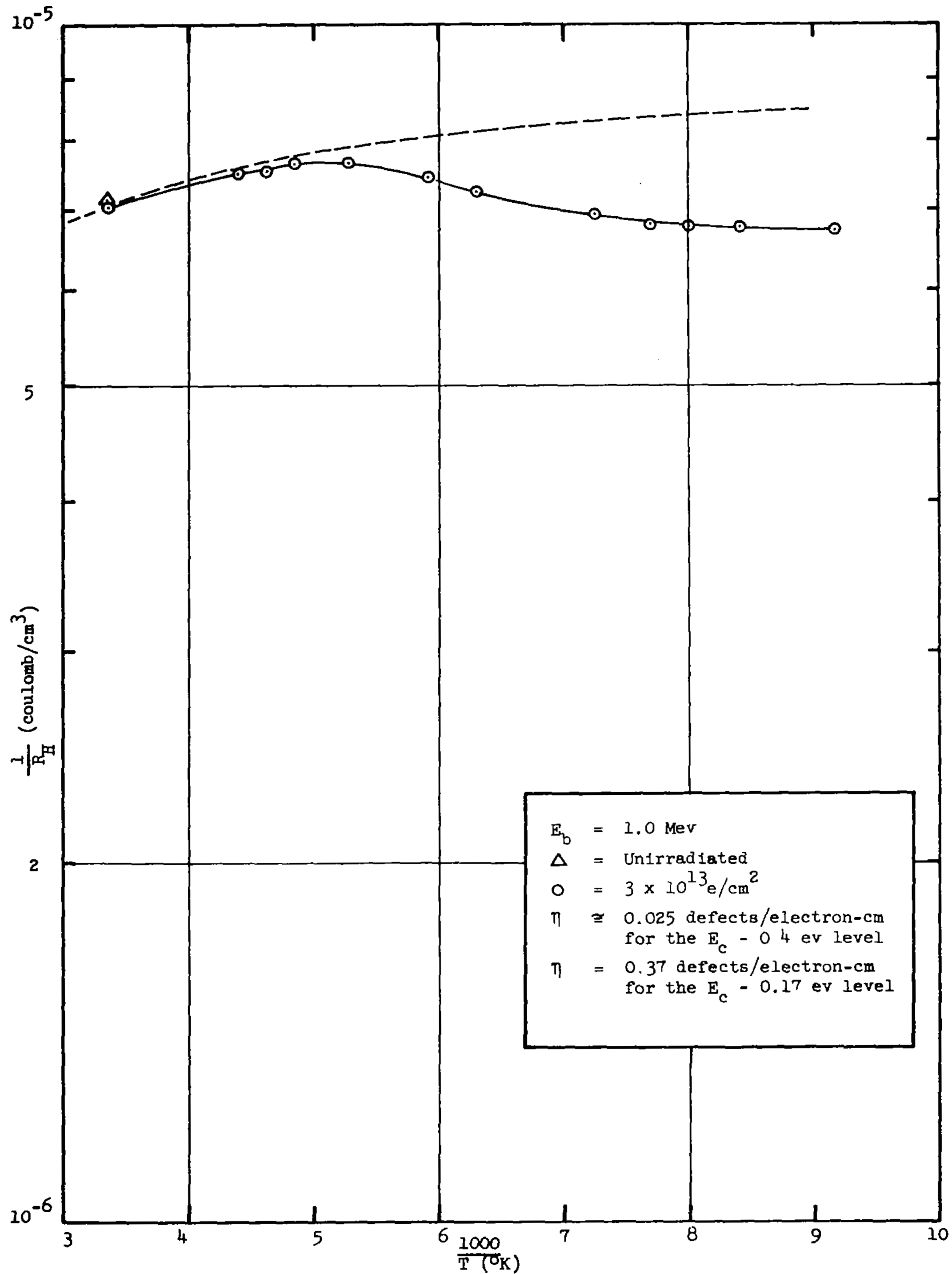

Figure 1. Temperature Variation of Reciprocal Hall Coefficient for 100 Ω -cm, n-type Silicon before and after Electron Irradiation (1.0 Mev)

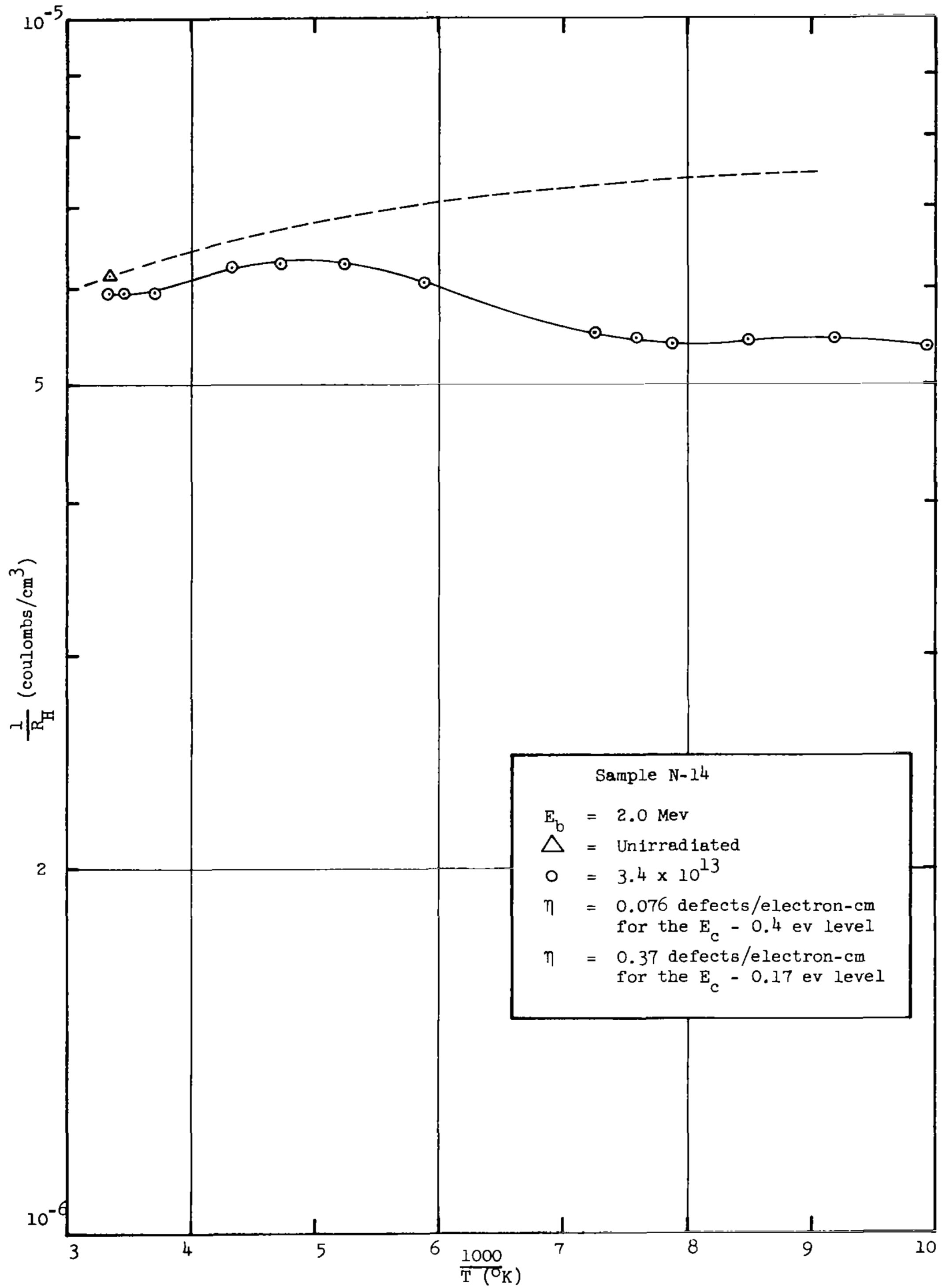

Figure 2. Temperature Variation of Reciprocal Hall Coefficient for 100 Ω -cm, n-type Silicon before and after Electron Irradiation (2.0 Mev)

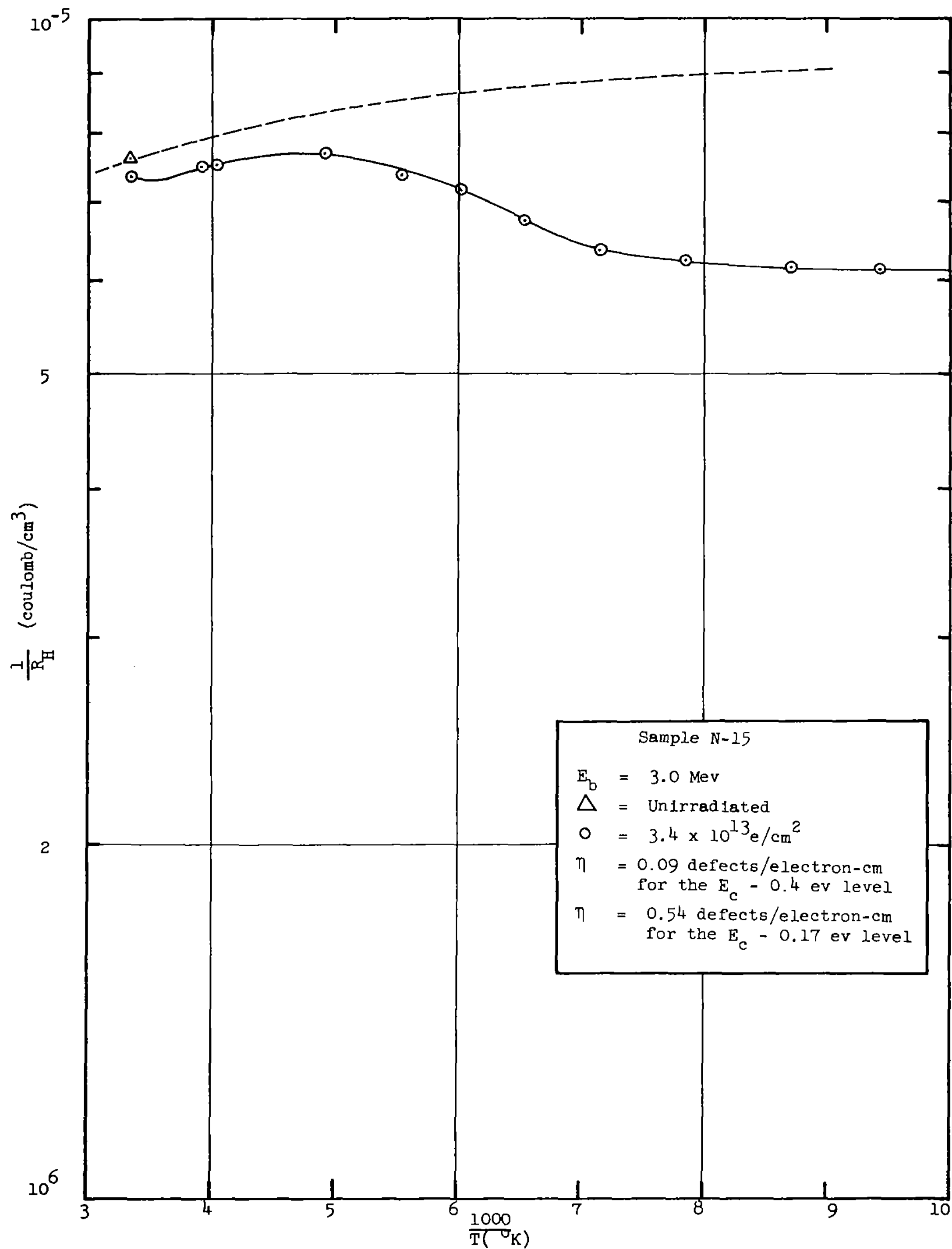

Figure 3. Temperature Variation of Reciprocal Hall Coefficient for 100 Ω -cm, n-type Silicon before and after Electron Irradiation (3.0 Mev)

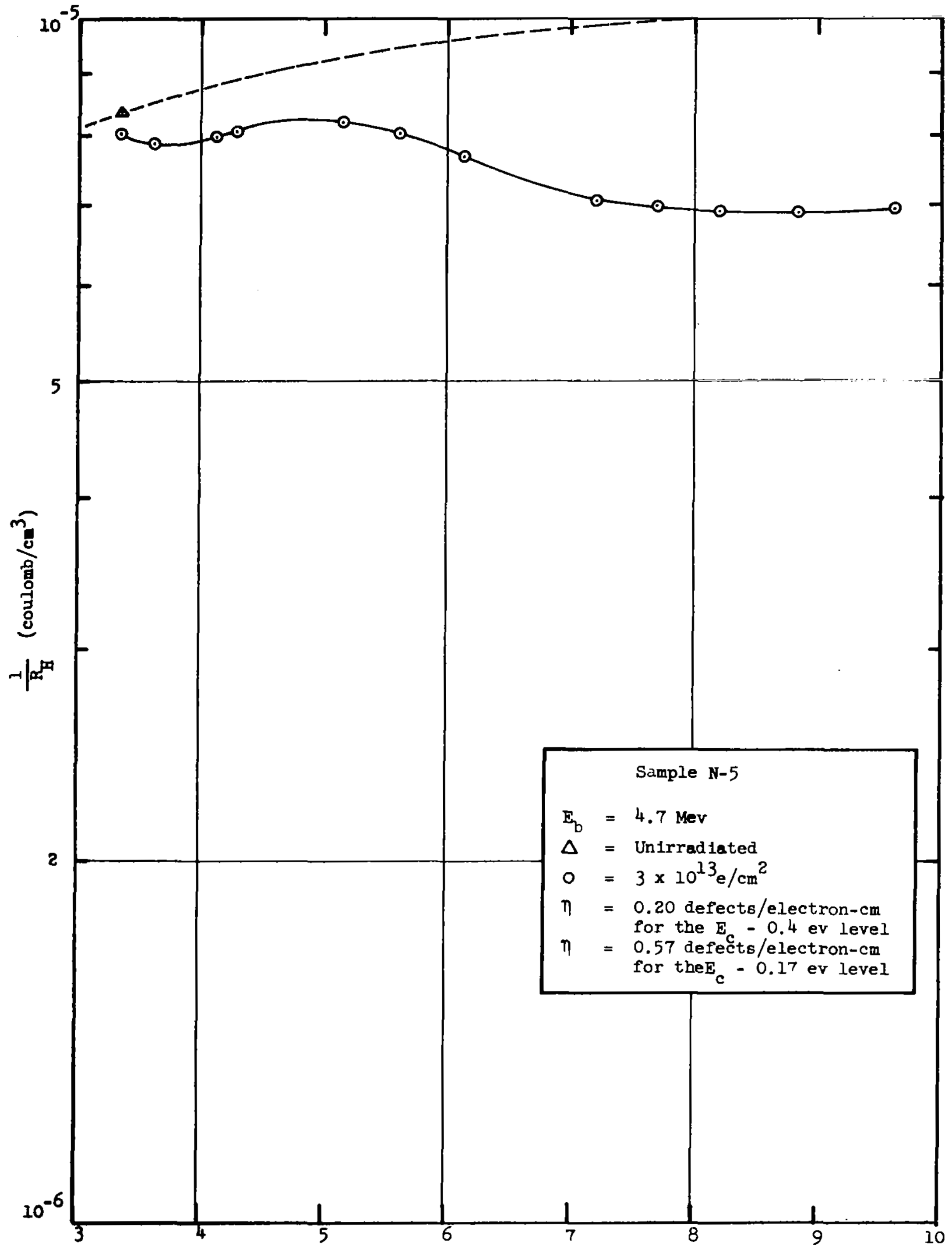

Figure 4. Temperature Variation of Reciprocal Hall Coefficient for 100 Ω -cm, n-type Silicon before and after Electron Irradiation (4.7 Mev)

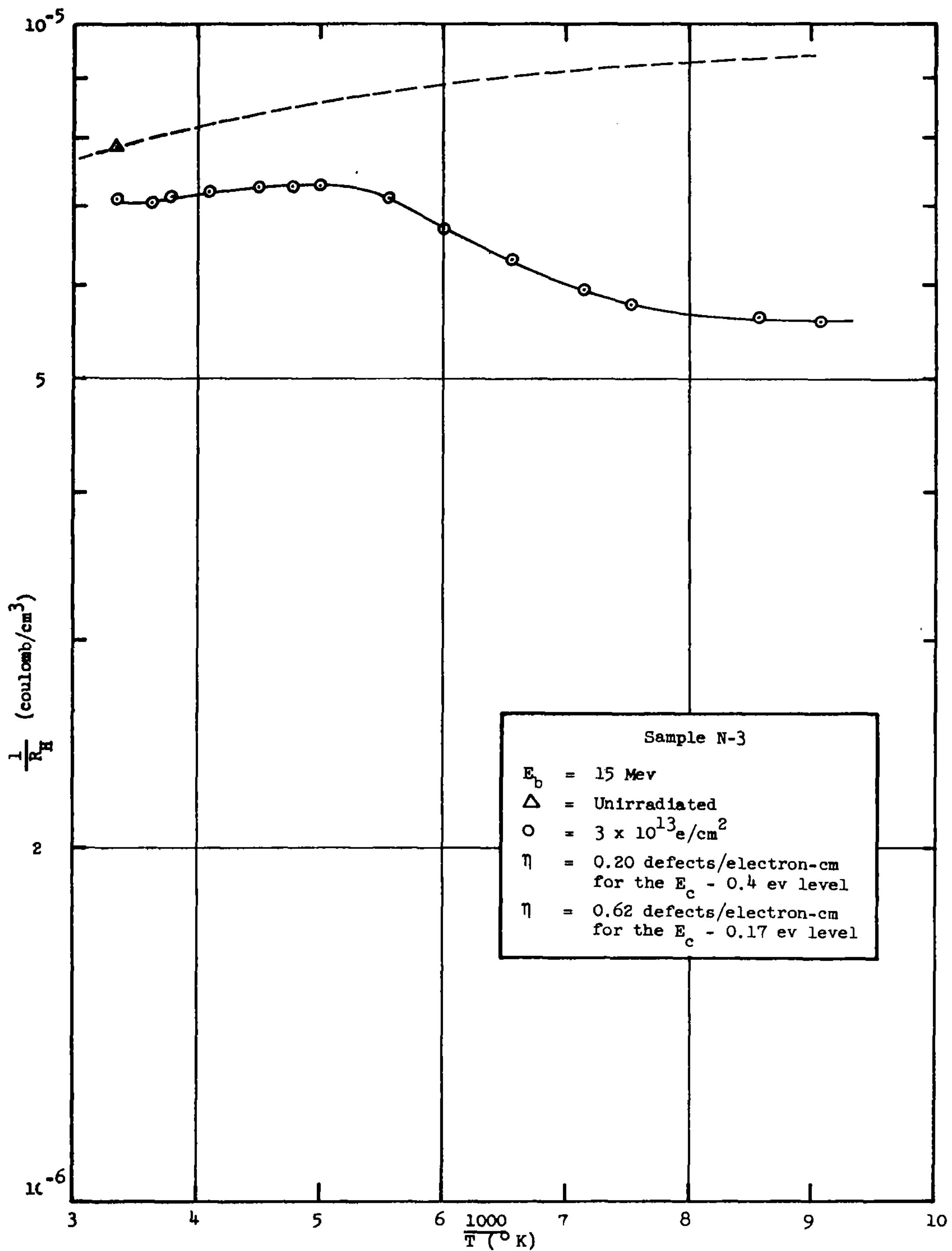

Figure 5. Temperature Variation of Reciprocal Hall Coefficient for 100 Ω -cm, n-type Silicon before and after Electron Irradiation (15 Mev)

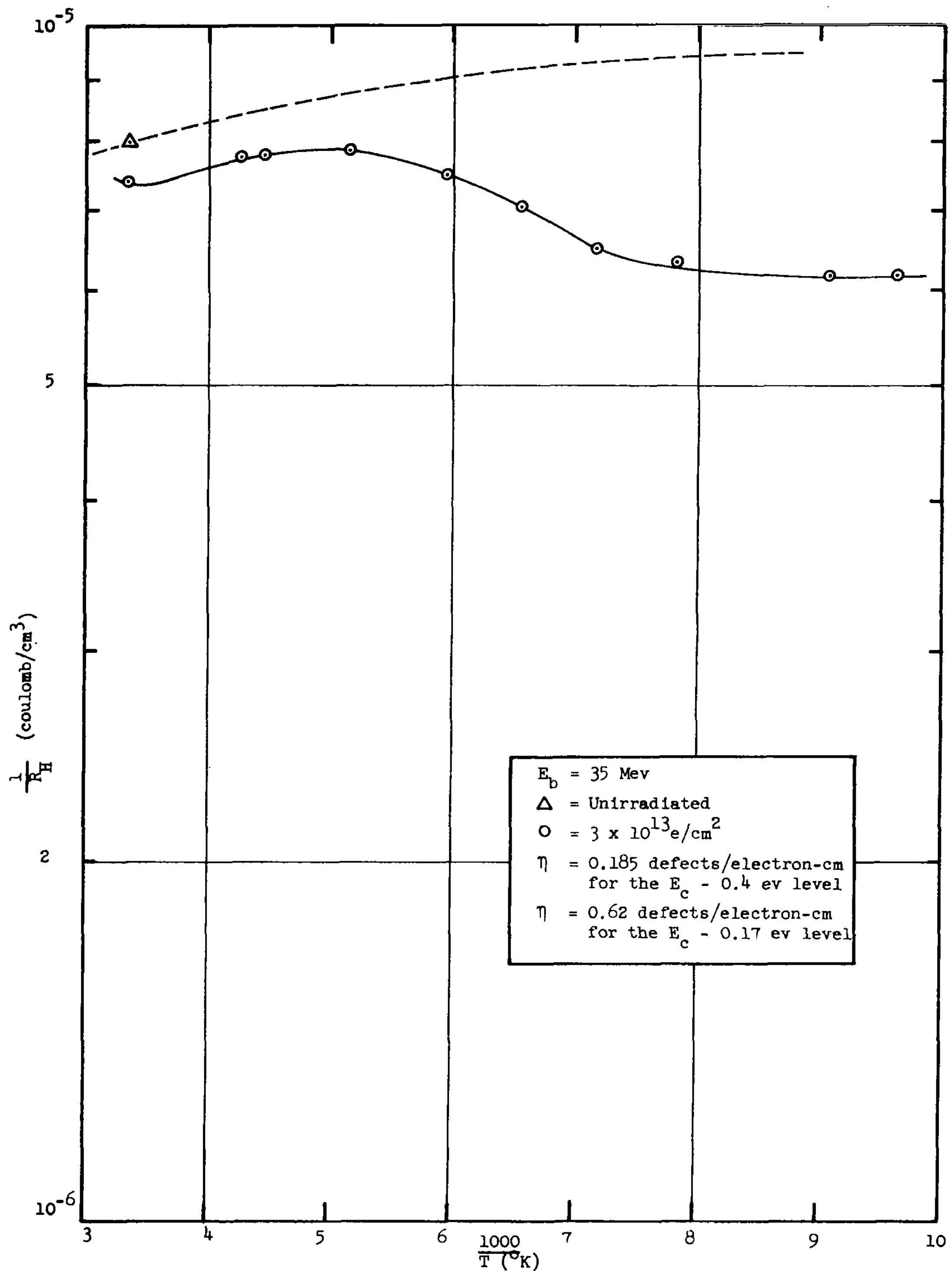

Figure 6. Temperature Variation of Reciprocal Hall Coefficient for 100 Ω -cm, n-type Silicon before and after Electron Irradiation (35 Mev)

above room temperature after irradiation. The data regarding introduction rates of these levels are summarized in Table I. The electron energy variation of η for the E_c - 0.17 ev and E_c - 0.4 ev levels is shown graphically in Figure 7. It can be seen that the introduction rates of these levels rise slowly for electrons above 1 Mev. Some data are included for 1 ohm-cm samples. The differences in η observed with varying resistivity are comparable to the amount of scatter in the data.

Figures 8 through 11 indicate the Hall coefficient analysis for p-type silicon irradiated with electrons of 0.7 Mev to 11.5 Mev. The data show evidence of only one level at E_v + 0.3 ev. The introduction rate of this level is increased greatly as the energy of the bombarding electrons increases. The data regarding introduction rate of this level are summarized in Table I. In general it appears that the introduction rates are functions of both dopant concentration and electron energy. The p-type data are summarized graphically in Figure 12. It can be seen that in all cases the introduction rate of the E_v + 0.3 ev level rises very rapidly with increasing electron energy. The shape of this curve depends to some degree on the resistivity of the silicon. The solid line represents only data from 15 ohm-cm silicon. The data from 75 and 130 ohm-cm vary in regard to shape and slope of the curve.

C. Discussion

A theory of displacements of solid atoms by fast electrons has been presented by Seitz and Koehler[15]. The concentration of displaced atoms is as follows:

$$n_d = \Phi \, n_o \, \sigma \, \bar{\nu} \qquad (3)$$

where n_d = concentration of defects

Φ = integrated electron flux

n_o = concentration of atoms in solid per unit volume

σ = displacement cross section

$\bar{\nu}$ = average secondary displacements per primary displacement

TABLE I

Summary of Data

Sample No.	ρ(ohm-cm, type)		E_b(Mev)	Φ(e/cm^2)	E_d(ev)	η(def/elec-cm)
N-18	100	n	0.6	$5x10^{13}$	E_c-0.17	0.30
N-11	100	n	1.0	$3x10^{13}$	E_c-0.4	0.025
					E_c-0.17	0.37
N-14	100	n	2.0	$3.4x10^{13}$	E_c-0.4	0.076
					E_c-0.17	0.37
N-15	100	n	3.0	$3.4x10^{13}$	E_c-0.4	0.09
					E_c-0.17	0.54
N-5	100	n	4.7	$3.0x10^{13}$	E_c-0.4	0.20
					E_c-0.17	0.57
N-3	100	n	15.0	$3.0x10^{13}$	E_c-0.4	0.20
					E_c-0.17	0.62
N-1	100	n	35.0	$3.0x10^{13}$	E_c-0.4	0.18
					E_c-0.17	0.62
N-100	1	n	1	$1x10^{16}$	E_c-0.17	0.30
N-101	1	n	3	$3.4x10^{15}$	E_c-0.4	0.11
					E_c-0.17	0.37

TABLE I

Summary of Data Continued

Sample No.	ρ (ohm-cm, type)		E_b (Mev)	Φ (e/cm^2)	E_d (ev)	η (def/elec-cm)
P-112	15	p	0.7	$2x10^{16}$	E_v+0.3	0.013
P-107	15	p	1.0	$9x10^{15}$	E_v+0.3	0.025
P-101	15	p	3.0	$2.3x10^{15}$	E_v+0.3	0.12
P-103	15	p	3.0	$4.6x10^{15}$	E_v+0.3	0.12
P-108	15	p	11.5	$4x10^{14}$	E_v+0.3	0.35
P-109	15	p	11.5	$1x10^{15}$	E_v+0.3	0.31
P-15	75	p	1.0	$2.0x10^{15}$	E_v+0.3	0.038
P-17	75	p	2.0	$1.16x10^{15}$	E_v+0.3	0.09
P-25	75	p	11.5	$1x10^{14}$	E_v+0.3	0.34
P-105-1	130	p	1.0	$1x10^{15}$	E_v+0.3	0.033
P-13	130	p	3.0	$3.4x10^{14}$	E_v+0.3	0.11
P-14	130	p	3.0	$5.7x10^{14}$	E_v+0.3	0.11
P-14	130	p	3.0	$5.7x10^{14}$	E_v+0.3	0.11
P-8	130	p	4.7	$2x10^{14}$	E_v+0.3	0.17
P-6	130	p	15	$1.5x10^{14}$	E_v+0.3	0.28
P-3	130	p	35	$1.2x10^{14}$	E_v+0.3	0.31
P-1	130	p	35	$7x10^{14}$	E_v+0.3	0.32

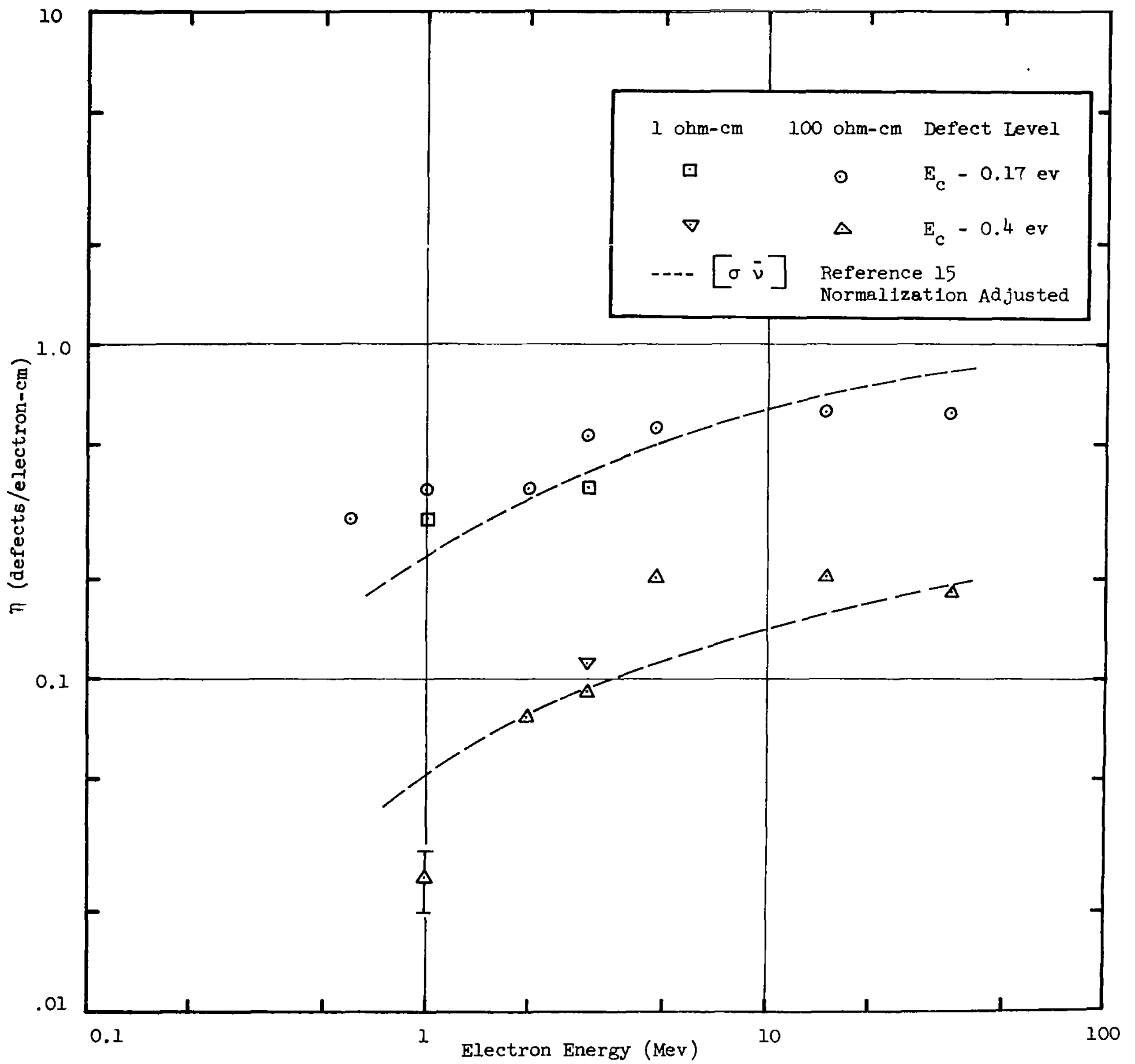

Figure 7. Introduction Rate of the E_c - 0.4 ev and E_c - 0.17 ev Levels in n-type Silicon for Electrons of Various Energies

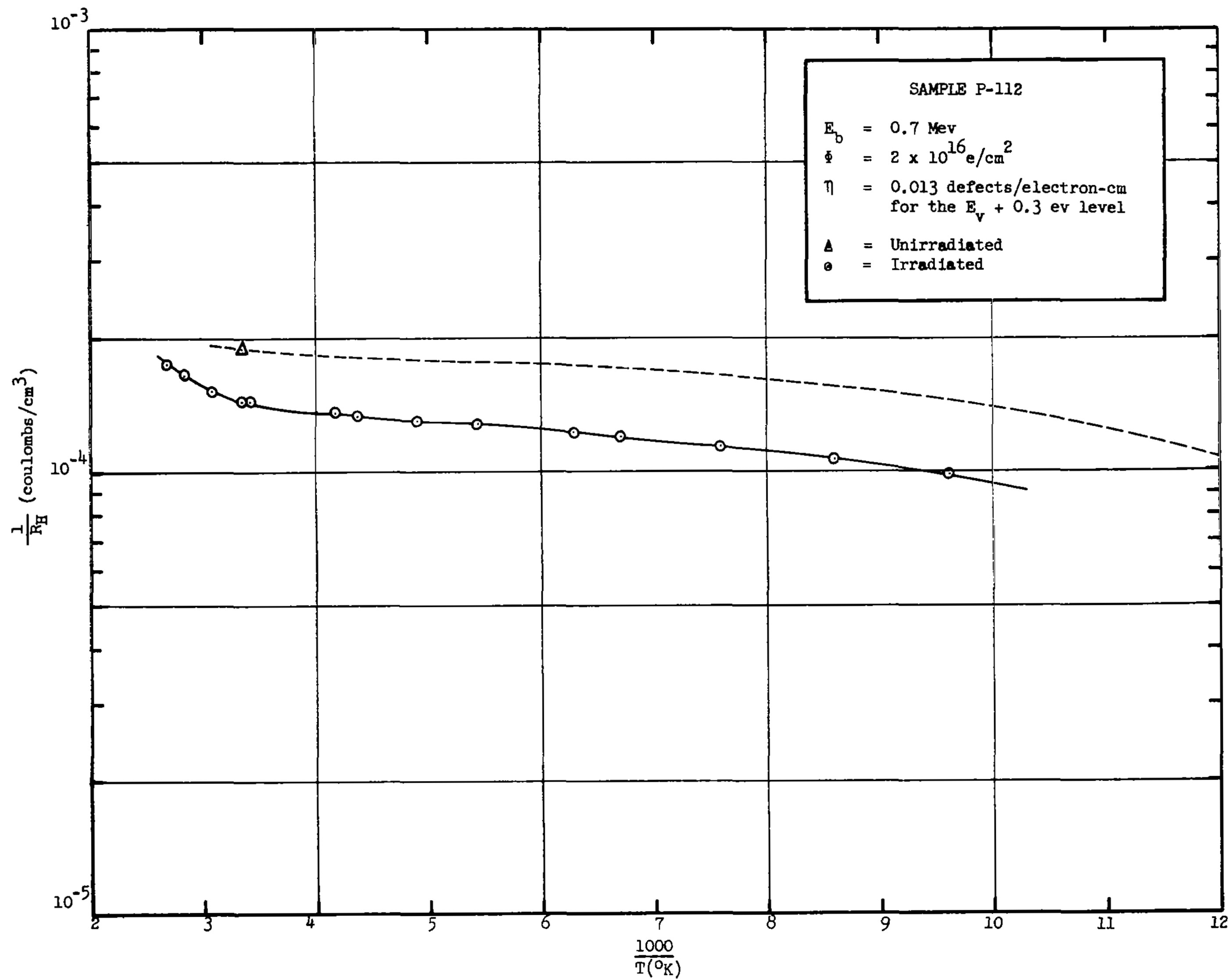

Figure 8. Temperature Variation of Reciprocal Hall Coefficient for 15 ohm-cm p-type Silicon Before and After Electron Irradiation (0.7 Mev)

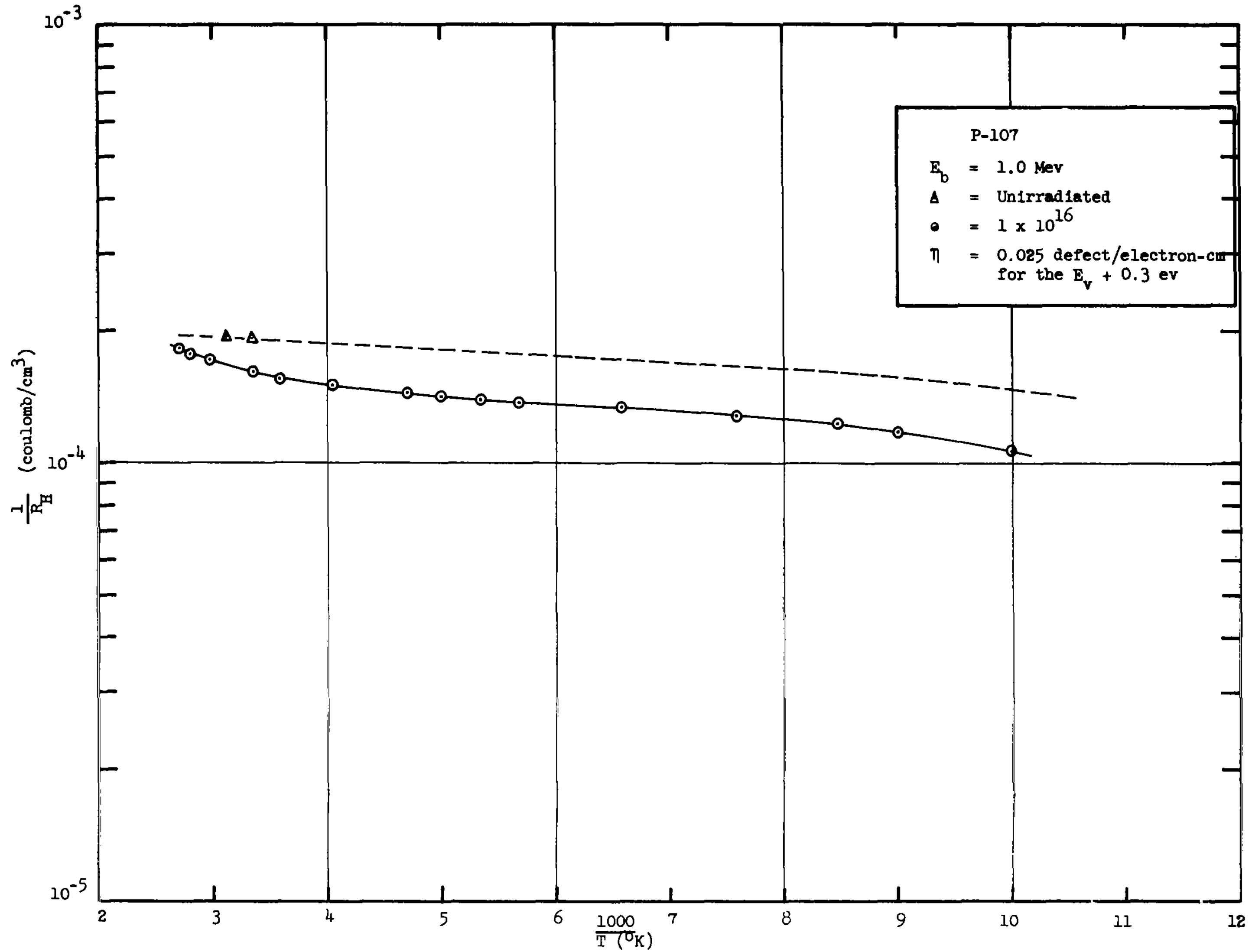

Figure 9. Temperature Variation of Reciprocal Hall Coefficient for 15 ohm-cm p-type Silicon Before and After Electron Irradiation (1.0 Mev)

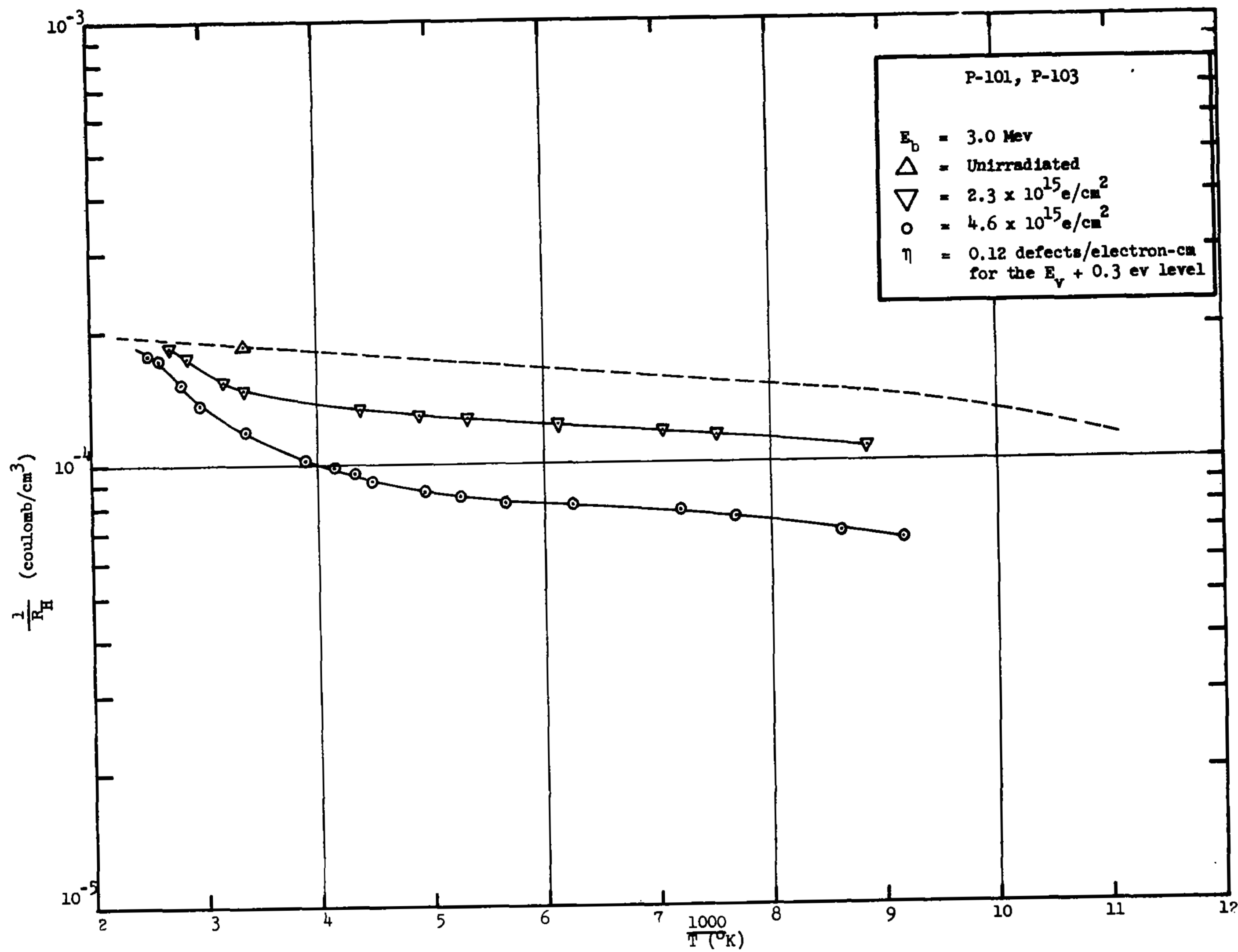

Figure 10. Temperature Variation of Reciprocal Hall Coefficient for 15 ohm-cm p-type Silicon Before and After Electron Irradiation (3.0 Mev)

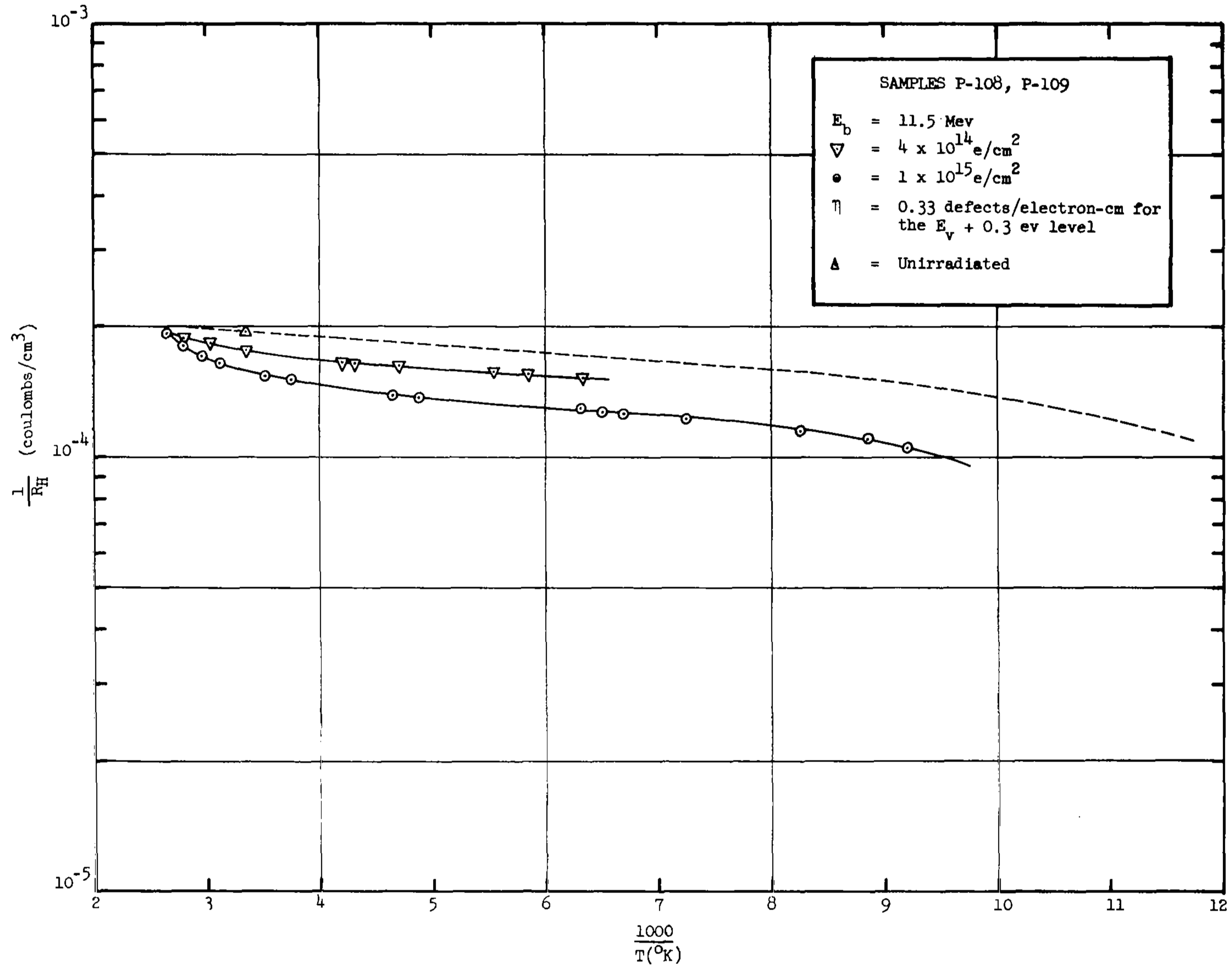

Figure 11. Temperature Variation of Reciprocal Hall Coefficient for 15 ohm-cm p-type Silicon Before and After Electron Irradiation (11.5 Mev)

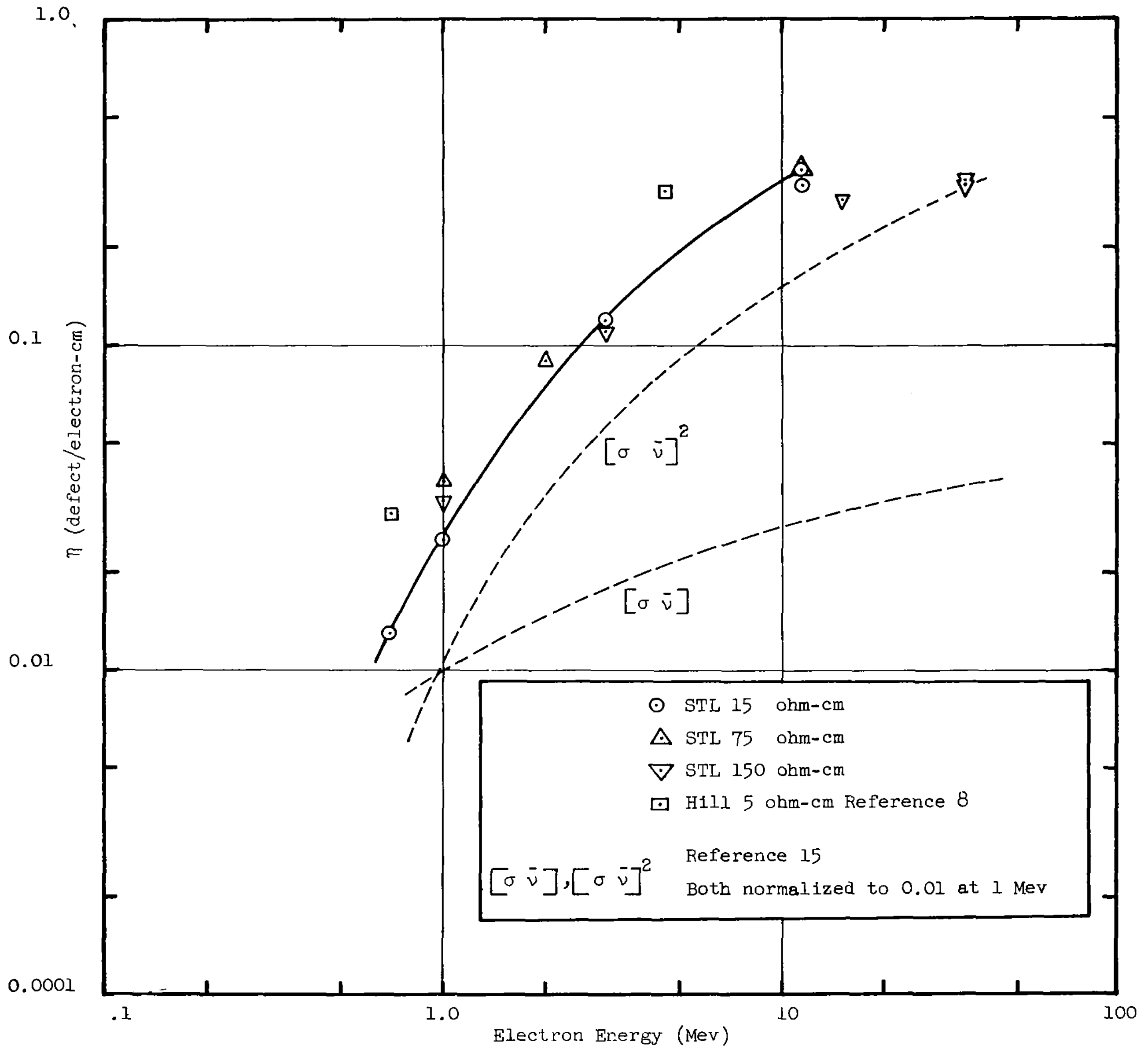

Figure 12. Introduction Rate of the E_v + 0.3 ev Level in Silicon for Electrons of Various Energies

Since a displacement involves production of a lattice vacancy and an interstitial, n_d should equal the concentration of vacancies or the concentration of interstitials produced by the irradiation. Typically, the values of n_d that one calculates are greater by an order of magnitude or more than the concentrations of defects detected. The physical structures of the defects reported here are known to be complexes involving vacancies and other chemical species rather than simple vacancies and interstitials. It appears that vacancies are involved in many solid state reactions such as:

V + I = lattice (a)

V + O = V-O, Si-A center (b)

V + P = V-P, Si-E center (c)

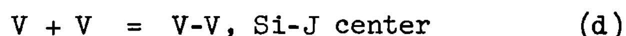
V + V = V-V, Si-J center (d)

where V = a silicon lattice vacancy
I = a silicon lattice interstitial
O = an oxygen atom
P = a phosphorus atom

Reaction (a) above probably accounts for the low concentration of defects compared to the theoretical concentration of displacement produced vacancies. It also can be assumed that the introduction rate of defects involving one vacancy (A or E center) should be proportional to the calculated introduction rate of vacancies or to $\sigma \bar{\nu}$. The extent of this agreement can be seen in Figure 7. Normalized plots of $\sigma \bar{\nu}$ have been fitted to the data on Figure 7. Although considerable scatter is observed, there is a very rough agreement between the energy variation of $\sigma \bar{\nu}$ and η for the E_c - 0.17 ev level. A similar agreement is found for the E_c - 0.4 ev level, however, at 1 Mev the agreement is very poor. It is also interesting to note that the energy variation of damage constant (K) and reciprocal critical flux (Φ_c^{-1}) for p on n solar cells has previously been reported to have the same energy variation as $\sigma \bar{\nu}$.[7]

The introduction rate of the E_v + 0.3 ev is contrasted to the other levels by a very fast rise in the electron energy range investi-

gated. This level may be associated with a divacancy.[16] A divacancy is thought to be two lattice vacancies on nearest neighbor sites. Such a defect may be formed by the diffusion of single vacancies to a site where two of them may react to form a divacancy. An alternate formation could occur by the primary displacement of a silicon atom followed by the secondary displacement of a nearest neighbor silicon atom. The first silicon atom must retain enough energy, after collision with the second, to avoid being trapped on the site of the second silicon atom. This double displacement also should be characterized by a higher threshold energy. This process is distinct from the earlier only in that the secondary displacement must occur on a nearest neighbor site to primary displacement. If the secondary displacement occurs on a next to nearest neighbor or more distant site with subsequent reaction of vacancies, the formation is limited by solid state diffusion or some other thermally activated process. If such a defect is formed by the reaction of two radiation produced vacancies, simple mass action principles indicate that the introduction rate of divacancies should be proportional to the second power of $\sigma \bar{\nu}$. A plot of $\sigma \bar{\nu}$ and $(\sigma \bar{\nu})^2$ is also shown on Figure 12. Both functions have been normalized to a value of 0.001 for 1 Mev. Since their shapes on the log-log plot are similar, it appears that the introduction rate of the E_v + 0.3 ev level in 15 ohm-cm silicon has the same energy variation as $(\sigma \bar{\nu})^2$. It is also obvious that the defect introduction rate in the 75 and 130 ohm-cm silicon are not following this relationship closely. The reasons for these deviations are unknown, but this difference in resistivity involves roughly an order of magnitude change in dopant concentrations. Such a change could involve considerable shift between competing reactions involving vacancies. If the divacancies are formed by double displacement with a threshold energy of roughly 50 ev and if the Seitz and Koehler analysis is applicable, the "double displacement" cross section will not be changed greatly for electron energies above 1 Mev. This is in direct contradiction to the data reported here for the E_v + 0.3 ev level.

The behavior of the E_v + 0.3 ev level was recently compared to that of the Si-K center in recent work at RCA.[17] The K center reportedly

is the dominant paramagnetic defect center in low resistivity p-type silicon. The structure of the K center is not known, however, the introduction rate increase with electron energy for this center is similar to that of the E_v + 0.3 ev level. The model suggested for the K center is a substitutional oxygen atom bonded to an interstitial silicon atom in the next to nearest site. This proposed defect could be formed by the reaction of a vacancy and an interstitial with an oxygen atom. The sequence of these events could be such that the formation rate would be proportional to the product of the concentration of vacancies and the concentration of interstitials. Since the concentration of vacancies should be directly related to the concentration of interstitials, this defect introduction rate could also be related to the second power of $(\sigma \bar{\nu})$.

An interesting similarity can be noted in the degradation of n on p silicon solar cells. Figure 13 shows experimental data from Reference 7 regarding the variation of the reciprocal critical flux of various n on p solar cells under electron irradiation of varying energy. These data also fit the energy variation of $(\sigma \bar{\nu})^2$. Since the resistivities used in these devices compare with the 15 ohm-cm p-type material studied in this work, it is interesting to note that the electron energy dependence of the Φ^{-1} and η are the same. Although this is not conclusive evidence, it indicates that the E_v + 0.3 ev level may be the recombination center in electron irradiated n on p silicon solar cells. The fact that the solar cell data follow the square power relationship also supports this theory, since degradation by the formation of J or K centers (E_v + 0.3 ev) could occur in this manner. This evidence is in direct contrast to previous studies of recombination centers in irradiated p-type silicon, where the most commonly suggested recombination center for electron damaged p-type silicon is the E_c - 0.17 ev level (A center). Electrons in the 1 Mev and lower range were used in these previous studies. The data presented here make it difficult to rationalize the E_c - 0.17 level or A-center as the recombination center in case of electron energies greater than 1 Mev. The damage rate of n on p cells rises much faster with energy than either the experimentally measured introduction rates of the E_c - 0.17 ev level or the theoretically expected rate $(\sigma \bar{\nu})$.

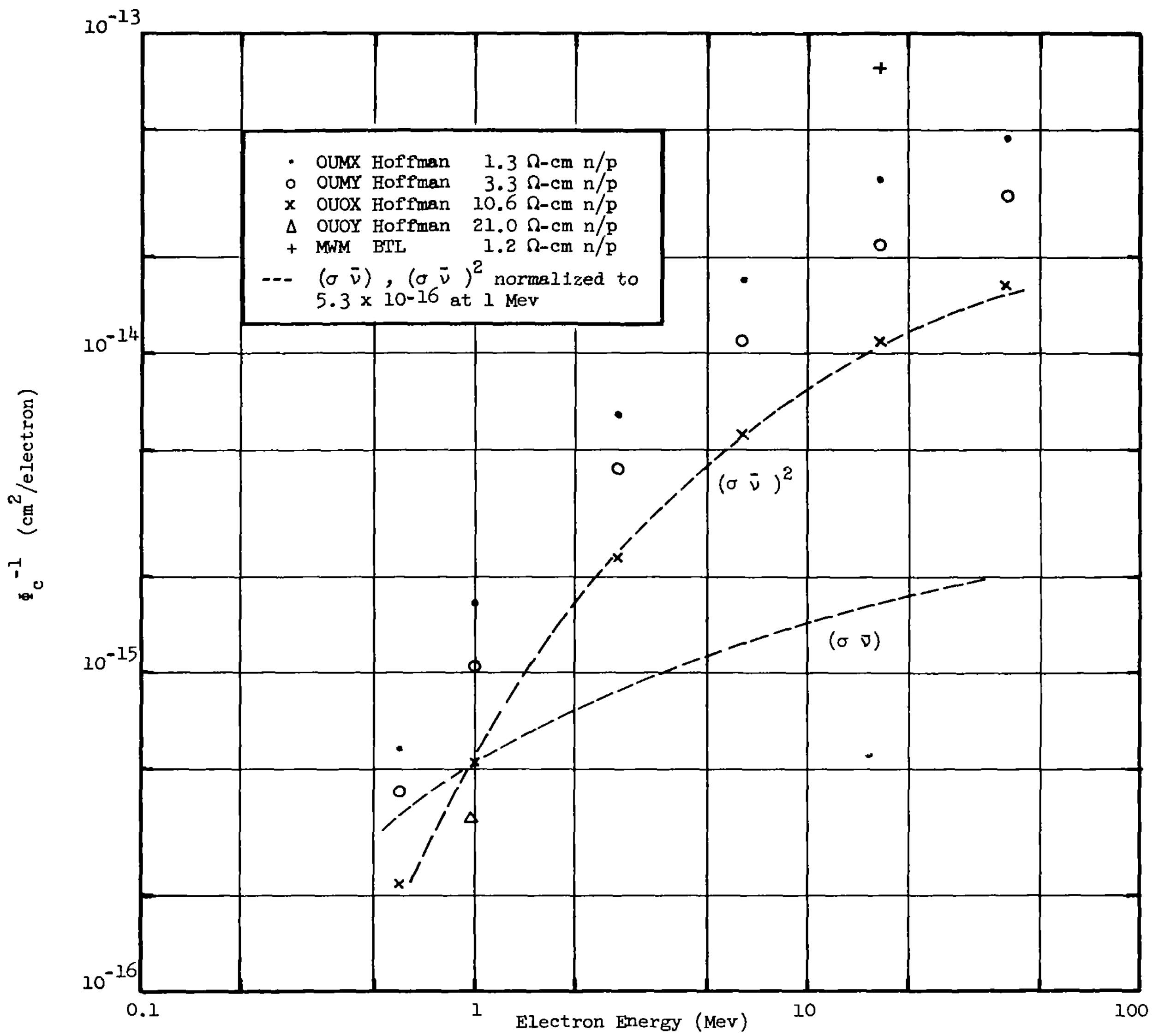

Figure 13. Electron Energy Dependence of Φ^{-1} Values for n on p Silicon Solar Cells

D. Conclusions

The phenomena of radiation induced defect levels in silicon is complex and difficult to understand. A considerable amount of reported experimental data is in direct conflict while other portions of the reported data seem to substantiate current defect models. The data and results presented in this report support the following conclusions:

1. The E_c - 0.17 ev and the E_c - 0.4 ev level introduction rates (η) raise very slowly for increasing electron energy above 1 Mev.
2. The η for the E_v + 0.3 ev level increases very rapidly with increasing electron energy.
3. The η of the E_v + 0.3 ev level and damage rate of n on p solar cells, as shown by Φ_C^{-1} and K values have identical energy dependence.
4. The energy dependence of η for the E_v + 0.3 ev level, and K values and Φ_C^{-1} for n on p silicon solar cells appear to be proportional to the second power of $(\sigma \bar{\nu})$. This similarity suggests that the E_v + 0.3 ev level and the recombination center in high energy electron irradiated n on p silicon solar cells are associated with a divacancy or other double displacement type defect.

Several points regarding E_v + 0.3 ev level remain unresolved. If this level is associated with the divacancy it should have the same η as that measured by ESR technique. The η for divacancies values reported by Corbett and Watkins[16], and Benski, "et al."[11] are lower than those of the E_v + 0.3 level by one and two orders of magnitude respectfully. In addition, preliminary annealing studies indicate that the E_v + 0.3 ev level does not anneal rapidly in the 300-400°C as reported for divacancies[16] or for irradiated n on p solar cells.[18] The effect of resistivity on η for the E_v + 0.3 ev level is very difficult to explain. The production of divacancies should be relatively independent of impurity concentration and maintain the same energy dependence regardless of contamination.

III. LOW ENERGY PROTON DEGRADATION IN SILICON SOLAR CELLS

The energy spectrum of the trapped proton belt around the earth is normally considered to be of the order of E^{-3} to E^{-5}. Because of the steepness of this energy spectrum silicon solar cells, which are necessarily exposed, receive a considerable dosage of low energy protons. Thus it is important to understand the response of solar cells to these low energy protons. Since low energy protons are not considered penetrating radiation, the extrapolation of data obtained with penetrating radiation, i.e., high energy electrons or high energy protons, does not yield meaningful results. The principal reason that extrapolation from penetrating radiation is not valid is that low energy protons produce regions of severe damage near the surface at depths less than a minority carrier diffusion length. Hence, the recombination of carriers in their process of diffusion to the junction becomes a complicated function in that the minority carriers will have different lifetimes depending upon the region in which they are diffusing. For these reasons, there is a great need for experimental information on the effects of low energy protons on silicon solar cells.

A. Experimental Techniques

During the course of this contract, two low energy proton experiments have been conducted; the first in December and January, the second in March. The facility utilized for these experiments was the STL 2 Mev proton Van de Graaff. Experiments were conducted at energies ranging from 0.2 Mev to 1.9 Mev. Due to the short range of protons of these energies in air, all of the experiments were conducted in a vacuum chamber. This chamber consisted of remote control apparatus for both mapping the beam and positioning test specimens in the beam. A shielded Faraday cup was used to determine the intensity of the beam as a function of position and to determine the total exposure of the test specimens by simultaneously irradiating the test specimen with the Faraday cup located in an adjacent position of equal intensity. The STL proton Van de Graaff facility does not incorporate the conventional HVEC magnetic analyzing

assembly. Hence, it was necessary to include in the chamber design a magnetic deflection system to separate the various components of the primary beam and remove all but the primary proton beam for the irradiations. The magnetic deflection system consisted of a 4" Varian magnet operated with flat 4" pole pieces and a one inch pole gap. Five distinctly separate identifiable beams were observed with this system; m_1, m_2, and m_3 beams at the principal operating energy as well as m_1 beams at one-half the principal energy and one-third the principal energy. These latter two beams are attributed to break-up of the m_2 and m_3 beams in the drift tube prior to entrance to the magnetic analyzer. The m_1 beam, referred to as the principal beam, consists simply of protons with a charge-to-mass ratio of 1. The m_2 beam with a charge-to-mass ratio of 1/2 is attributed to singly ionized hydrogen molecules which are not completely ionized at the source and are subsequently accelerated to the full potential. The m_3 beam with a charge-to-mass ratio of 1/3 is attributed to tri-atomic, singly ionized hydrogen molecules for which the formation mechanism is not well known. The m_1, m_2, and m_3 beams were present in the primary beam with about equal magnitudes while the 1/2 and 1/3 principal energy m_1 beams were about two orders of magnitude less in intensity. Scatter shields were included in the irradiation chamber to effectively remove the unwanted beam components after magnetic analysis. Experiments were performed at magnetic deflections of the principal beam of 10 and 20 degrees.

In order to investigate the beam, considerable beam analysis with a silicon solid state detector and a 400 channel pulse height analyzer was performed. It was observed that when very small entrance and exit apertures for the magnetic analyzer were used (0.1" or less) the analyzed beams were extremely clean with an energy width of the order of a few percent. Also, the principal beam comprised over 95 percent of the total number of particles incident on the detector. In this clean configuration, however, the beam diameter was too small to perform meaningful experiments on solar cells. Since no control over beam spot size could be exercised past the analyzing magnet, much larger apertures were

necessarily used to obtain sufficient beam diameters. It was observed, however, that as the analyzing apertures were made larger, the energy width and content of the beam deteriorated. For extremely large apertures the energy width of the beam would approach 30 to 40 percent and the content of the beam attributable to the principal beam was observed to drop to as low as 60 percent. As a result, it was necessary to compromise the irradiating beam content significantly in order to obtain reasonable beam diameters for the conduct of the irradiations.

The test specimens used in these experiments consisted of 1 ohm-cm, 1 cm x 1 cm p/n silicon solar cells and 10 ohm-cm, 1 cm x 1 cm n/p silicon solar cells, both types furnished by Hoffman Electronics Corporation. The bulk of the data was obtained for the 10 ohm-cm n/p cells since they are of principal practical importance; however, sufficient data was obtained for the p/n cells to ensure correlation. Junction depths of both types of cells were 0.5 microns while their initial efficiencies were of 8 to 10 percent. Measurements of I-V characteristics were performed using the STL sun simulator (an OCLI unit) and a 2800°K unfiltered tungsten light table. The tungsten light table used in these experiments is the same unit described in previous reports[19] on radiation damage and has been held at a constant intensity for the last four years through a series of standard cells. The sun equivalent power for this tungsten source will therefore vary slightly depending on the particular characteristics of the cells under test but usually lies between 130 mw/cm^2 and 140 mw/cm^2 for contemporary silicon solar cells.

B. Results

The analysis of the data to be presented in this section is based on radiation induced changes in the I-V characteristics as observed under both tungsten and sun illumination. Changes in short circuit current, open circuit voltage, and maximum power as a function of integrated proton flux and proton energy are the principal parameters studied and presented here. Changes in other important solar cell parameters such as series resistance, in-beam annealing, and rapid post-irradiation annealing were also

observed. Since, however, analysis of the data yielded no significant trends for these parameters, their inclusion in the results is necessarily limited to general mention and discussion.

The degradation of short circuit current density as a function of proton energy is shown in Figure 14. For each energy shown, 3 to 7 cells were used to obtain the data presented in this section. The data shown in Figure 14 indicate that in the low energy proton region the degradation rates, i.e, the slopes of the degradation curves, seem to vary considerably as a function of energy. The slopes all appear to be steeper than the normal 6.5 to 7 ma/cm^2 - decade observed for penetrating radiation of either electrons or protons. The slopes shown for 1.9 and 1.7 Mev appear to be approximately 10.5 ma/cm^2 - decade increasing to about 12 ma/cm^2 - decade at 1.5 Mev and 15.5 ma/cm^2 - decade at 1 Mev. At this point the slopes appear to start decreasing again indicating about 13 ma/cm^2 - decade at 0.5 Mev and considerably less than that at 0.3 and 0.2 Mev. The degradation rates at these latter two energies were so slow that inadequate beam time was available to obtain sufficient data for slope determination. A group of p on n cells were irradiated at 0.5 Mev for comparison with the n on p cells and, as shown in Figure 14, the degradation rates are identical. Sufficiently low beam intensities for the irradiation of p on n cells were difficult to obtain, and also since principal interest is in the n on p cells, a large amount of information was not obtained for p on n cells other than to verify that their response was similar in nature to the n on p cells. It is also observed in Figure 14 that the knee of the curve i.e., the point of the intersection of the slope with the initial conditions, seems to reach a minimum value somewhere between 1.9 Mev and 6.7 Mev and then reverses its direction toward higher values of integrated flux with further decrease in proton energy.

A series of post irradiation measurements indicated that considerable room temperature annealing occurs for low energy proton irradiated cells. Recovery of between 20 percent and 90 percent of the short circuit current was observed in times of the order of days. Annealing

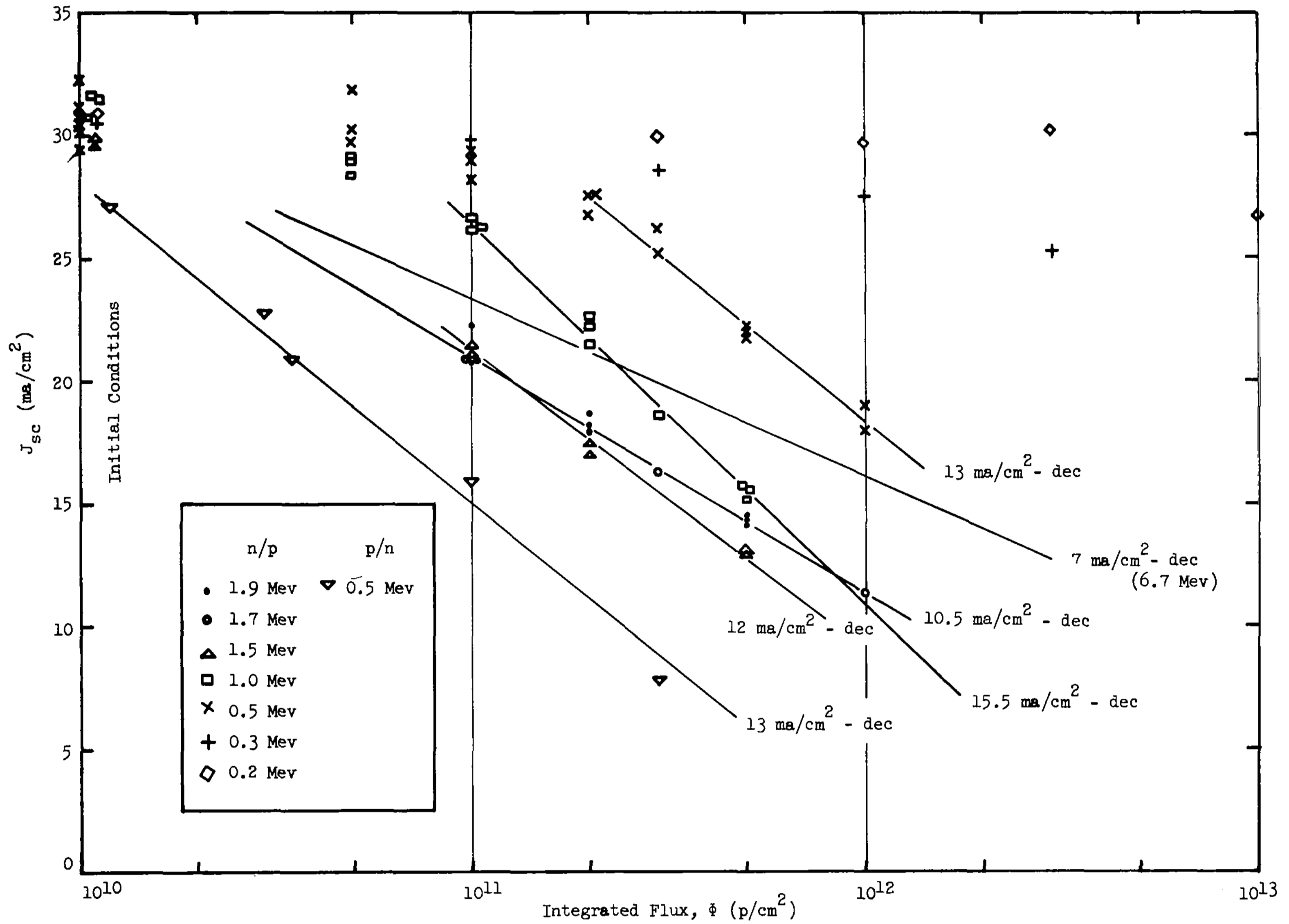

Figure 14. Silicon Solar Cell Short Circuit Current Degradation Under Low Energy Proton Irradiation

of open circuit voltage at room temperatures was not observed. There appeared to be no correlation, however, in the annealing data in that the observed recovery was not a consistent function of either proton energy, time, or amount of radiation induced damage. In addition to room temperature annealing, in-beam annealing was also observed. Although the beam intensities utilized in the experiment were not sufficiently high to raise the temperature of a solar cell it is quite probable that, due to the short range of the protons, localized heating in the region near the junction where the damage is occurring is responsible for the observed phenonema. In several cases for longer iriradiations at the same intensities, I-V curves were actually obtained wherein the open circuit voltage had proceeded with its normal degradation but the short circuit current had actually been annealed to a higher value than before the irradiation was initiated. For this reason, some of the short circuit current data at the higher fluxes were considered invalid and are therefore not shown on the plot of short circuit current versus integrated flux.

In order to obtain a comparison between observed degradation in short circuit current under tungsten illumination and equivalent performance under solar illumination in space, a series of measurements were made using the STL sun simulator which is an OCLI unit. The results of this comparison are shown in Figure 15. The typical response for penetrating radiation in the solar simulator versus our standard 2800°K tungsten source, which has been maintained constant over the past four years, is shown in the figure. The expected departure from this typical response is evident in that for the case of severe damage near the surface of the cell the degradation under sun illumination is more severe for the same degradation under tungsten illumination due to the higher blue content of solar illumination. However, there is no statistically significant difference observed for proton energies ranging from 0.5 to 1.9 Mev. Some difference would be expected in this range; however, the scatter in the data is apparently greater than the difference in response. On the other hand, a significant departure is observed for

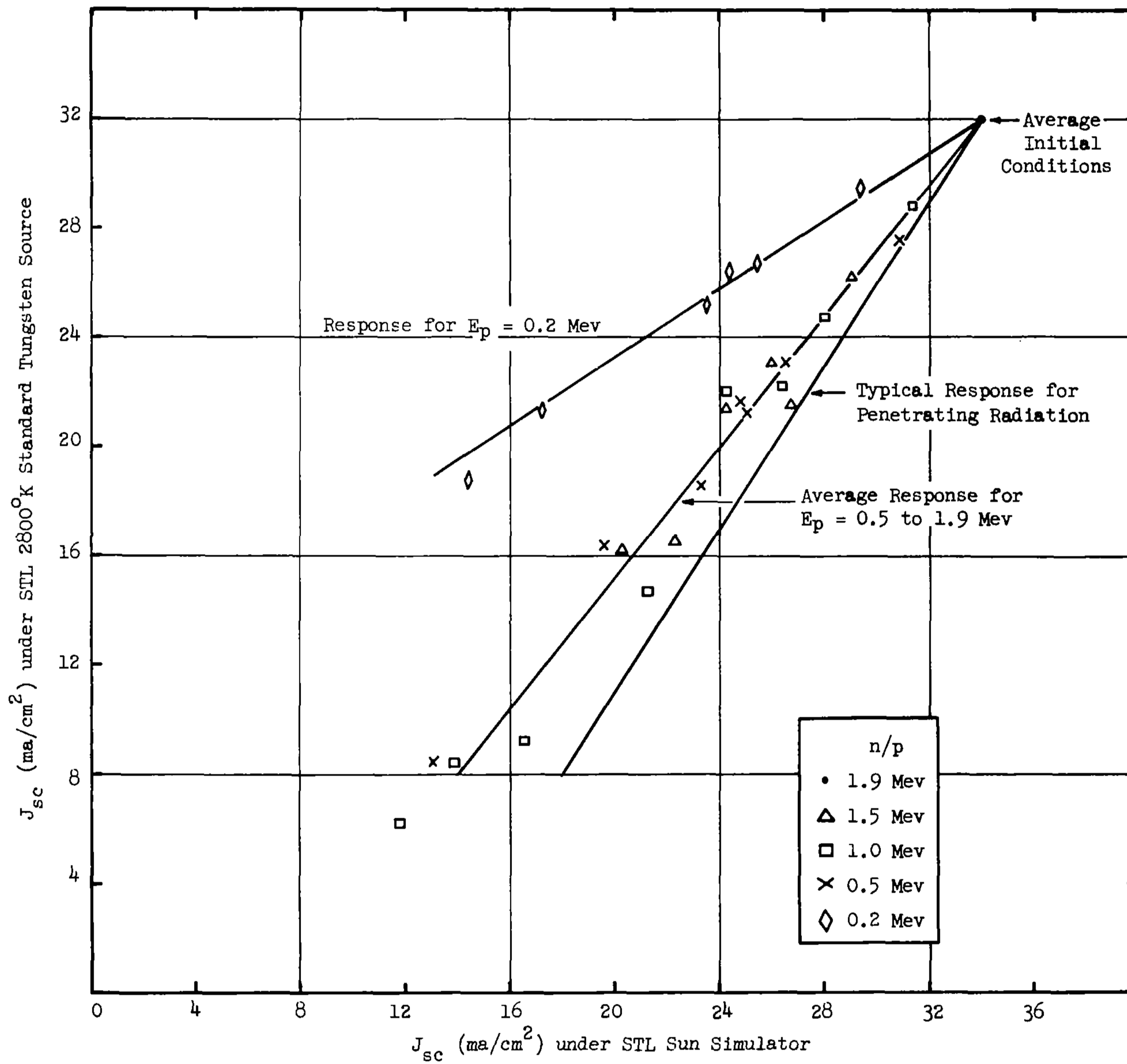

Figure 15. Comparison of Sun Simulator Data with 2800°K Tungsten Data

proton energies of 0.2 Mev indicating a rapid deterioration of response to the short wavelength component of solar illumination at energies below 0.5 Mev. These curves were used to calculate degradation of output power in space which will be presented in a later section.

Degradation in open circuit voltage versus integrated flux and proton energy is shown in Figure 16. The observed degradation rates, or slopes, are all approximately alike and equal to about 120 mv per decade. There appears to be slight deviations in this slope as a function of proton energy but these deviations are less than the scatter in the data and hence unresolvable. These slopes, however, are considerably greater than the slopes observed in the case of either electron or proton penetrating radiation wherein slopes of the order of 40 to 50 mv/decade are commonly observed for 10 ohm-cm n on p cells. Although examination of I-V characteristics as a function of proton energy seems to imply a greatly increasing sensitivity of open circuit voltage at the lower proton energies, this is not in actuality the case as evidenced by the data in Figure 16. The maximum sensitivity of the open circuit voltage seems to lie somewhere between 1.5 and 2 Mev with decreasing damage sensitivity at energies of 1 Mev and less. The illusion that the open circuit voltage degradation is increasing at energies of 1 Mev and below is due primarily to the fact that the short circuit current degradation sensitivity is decreasing very rapidly and in fact at lower energies the open circuit voltage is the principal degradation parameter. The shift from the 40 to 50 mv/decade degradation rate observed for proton energies as low as 6.7 Mev to the steep slopes shown in Figure 16 apparently occurs between 2 Mev and 6.7 Mev.

Due to the peculiar nature of the response of silicon solar cells to low energy protons, extrapolation of data for penetrating radiation to performance in space is not a valid approach. Therefore, the I-V characteristics obtained in these experiments were corrected for actual space conditions through the use of Figure 15 for further analysis. A plot of the degradation of P_{max} versus integrated flux was then obtained

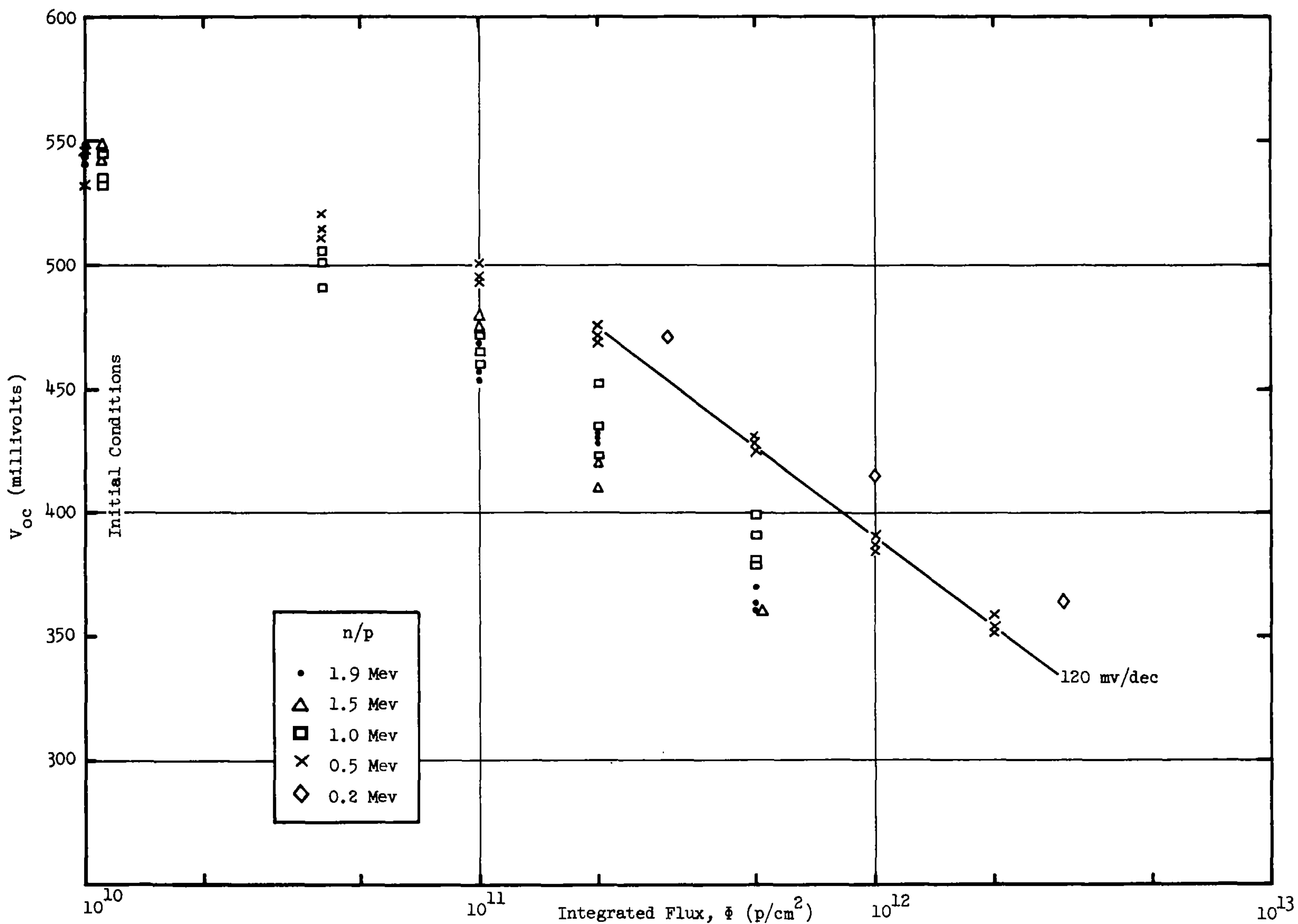

Figure 16. Silicon Solar Cell Open Circuit Voltage Degradation Under Low Energy Proton Irradiation

as shown in Figure 17. The degradation in P_{max} is observed to be maximum for proton energies of 1.5 and 1.9 Mev while falling off at energies of 1 Mev and below. In comparing this data with data previously obtained at 6.7 Mev it appears evident that the region of maximum over-all degradation in the power producing capability of silicon solar cells lies in the region of 2 to 6 Mev and is most probably quite close to 2 Mev. The slopes, as anticipated, are considerably steeper than those observed for penetrating radiation. In the case of penetrating radiation, degradation rates of approximately 20 percent per decade are commonly observed wherein the slopes observed for proton energies between 1.9 and 0.5 Mev are approximately 45 percent per decade. However, at 0.2 Mev the degradation rate appears to have decreased considerably due to the decreased sensitivity of the short circuit current degradation. The observed degradation at 0.2 Mev in these experiments is approximately 20 percent per decade in spite of the fact that at these lower proton energies observable degradation in the series resistance of the cell begins to become quite evident and important. Considering the wide variations in degradation rates observed for the short circuit current, the uniformity of the degradation rates for P_{max} is somewhat surprising and can only be accounted for by unresolvable differences in the degradation rates of other parameters such as open circuit voltage, series resistance, and short term annealing.

C. Conclusions

The degradation rates for the open circuit voltage, short circuit current, and P_{max} all increase substantially under low energy proton bombardment relative to degradation rates observed for penetrating radiation. In particular the short circuit current degradation rate seems to show a very strong dependence on proton energy in the region below 2 Mev. The net result of the degradation in the I-V characteristics is summarized by the degradation in the maximum power producing capability of the cell. Although the power degradation rate is almost twice as high as for penetrating radiation, maximum sensitivity seems to occur in a re-

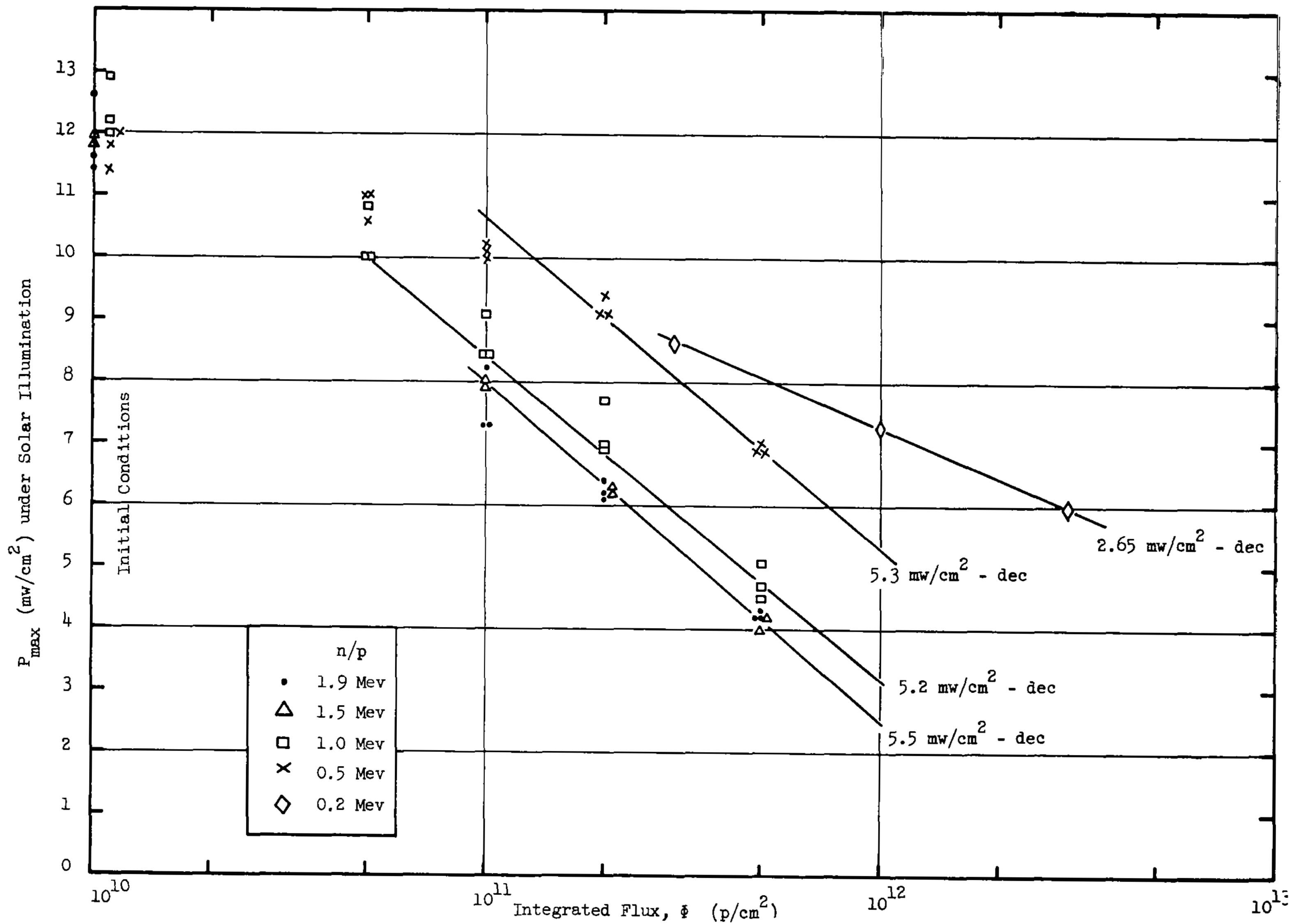

Figure 17. Degradation of Maximum Power Output for Silicon Solar Cells Under Low Energy Proton Irradiation

gion between 2 and 6 Mev and most probably very near 2 Mev. For an equal exposure of lower energy protons, the absolute power degradation decreases with further decrease in proton energy below 2 Mev. Hence, the proton radiation sensitivity of silicon solar cells which is increasing with decreasing proton energies seems to reach its maximum sensitivity in a region near 2 Mev and then begins to fall off. Inasmuch as the data shown here are presented as unannealed data, and since measurable annealing at room temperature for short periods of time has been observed, the actual power degradation experienced in space over a long period of time will not be as severe as indicated by these data.

Although considerable data were obtained in these experiments, it is difficult to assess a meaningful accuracy to the results due to the compromised proton beam ultimately used. It is estimated that the accuracy of the data is most probably good to within a factor of 2 but it cannot be considered accurate to within 5 or 10 percent. It is evident that considerably more effort needs to be expended in the acquisition of low energy proton data. However, a facility capability of a higher energy and a more complete magnetic analyzing system would be required to improve on the accuracy of the data and cover the range to at least 4 or 5 Mev.

IV. EFFECT OF IMPURITIES ON RADIATION DAMAGE IN SILICON

The effect of impurities on the electrical properties of semiconductor materials has long been known. It has been shown that the response of semiconductor materials in the presence of a radiation environment can be effected by the presence of either deliberately induced impurities or trace impurities which do not normally affect the material's characteristics in the absence of a radiation environment. For example, a group of silicon solar cells produced from oxygen free crystals exhibited a marked decrease in radiation sensitivity under 20 Mev proton bombardment.[20] Further experiments, however, with oxygen free silicon indicated that the observed decrease in radiation sensitivity could not be attributed to the oxygen concentration but rather to some other unidentified impurities present in that particular crystal.

It can be expected, therefore, that through the controlled use of impurities the response of silicon to radiation can be either reduced or enhanced. Particular identification of an impurity to reduce the sensitivity of minority carrier lifetime to high energy radiation has not yet been identified for silicon. Data have recently been presented[21], however, which suggests an apparent decrease in sensitivity of aluminum doped silicon. In order to obtain further information on the radiation sensitivity of aluminum doped silicon, a series of experiments were performed which are described in this section.

A. Experimental Techniques

In order to obtain an adequate measure of the sensitivity of minority carrier lifetime to high energy radiation, K values are used as an criterion of sensitivity. This technique is superior in the determination of absolute sensitivity than short circuit current since the short circuit current of a silicon solar cell is a function of many things which are not affected by radiation and can, therefore, induce considerable random variations in the data. The techniques for obtaining K values

have been previously described[19] but will be reviewed briefly here. The minority carrier diffusion length of irradiated silicon can be expressed as:

$$\frac{1}{L^2} = \frac{1}{L_o^2} + K\Phi \qquad (4)$$

where L = the final minority diffusion length

L_o = the initial minority diffusion length

Φ = the total integrated flux

K = the damage constant

The use of this equation requires that the defect introduction rate remain constant and that other characteristics of silicon which effect minority carrier lifetime, such as resistivity, also remain constant. If these conditions prevail, then a log-log plot of minority carrier diffusion length versus integrated flux will have a slope of minus 0.5. Under these conditions K is a constant and can be used as a measure of the sensitivity of the material as expressed by:

$$K = (L^2 \Phi)^{-1}, \text{ for } L << L_o \qquad (5)$$

It must be remembered that K is constant only if the slope of the minority degradation characteristic is equal to a minus 0.5. In a majority of the data obtained for K values the observed slopes will fit a minus 0.5 slope within the statistical variations of the data or unless the total integrated flux becomes sufficiently high to effect changes in the material resistivity. In some cases, significant departures can be observed for specific groups of cells; however, such departures are observed only occasionally and have never exceeded a slope of 0.4. The I-V characteristics for the cells were measured with the 2800^oK tungsten light table which was described in Section III-A. From these I-V characteristics degradation of short circuit current was also obtained for comparison with K values.

The test specimens consisted of two separate lots of silicon solar cells furnished by Texas Instruments. Each lot was broken

up into five cells of four different types of base material described as follows:

Group 1 (5 cells)

1 x 2 cm, 5 grid, 15 mil thick blanks, pulled crystal boron doped, Ti-Ag contacts, 1.5 - 3.0 ohm-cm base resistivity.

Group 2 (5 cells)

Same as above, except 10 - 12 ohm cm base resistivity.

Group 3 (5 cells)

Same as above, except Aluminum doped crystal and 1.5 - 3.0 ohm cm base resistivity.

Group 4 (5 cells)

Same as Group 3, except 10 - 12 ohm cm base resistivity.

The two lots were obtained at different times and hence will reflect any changes in sensitivity due to time dependent variations in manufacturers production lines techniques.

B. Results

After receipt of the first lot of cells the irradiations were initiated on four specimens from each group maintaining one cell as a control. After a total dose of 2×10^{14} e/cm^2 an equipment malfunction in the electron beam dosimetry electronics was detected. This failure invalidated all the data acquired to that point. At this time, the second lot of cells was requested and furnished by Texas Instruments. Upon receipt of the second lot of cells, the test was reinitiated using all of the cells from the second lot and the control cell from the first lot. In addition, the remaining cells from the first lot which had already received 2×10^{14} e/cm^2 were irradiated to an integrated flux 2×10^{15} e/cm^2 at which point the effect of the initial tests would be negligible in the analysis.

The degradation of short circuit current for the 1 ohm-cm cells is shown in Figure 18. The data indicates that in the second lot of cells the aluminum doped silicon is approximately a factor of 2 better than the boron doped cells, whereas, in the first lot the aluminum doped cells did not exhibit as strong a difference in response. The 1 ohm-cm boron doped cells for the two lots are practically identical. In Figure 19 the degradation in minority carrier diffusion length is shown as a function of integrated flux. As evidenced in Figure 19 the aluminum doped cells exhibited a somewhat better resistance than did the boron doped cells for the second lot; however, the first lot indicated exactly the reverse, in that the boron doped cells were almost a factor of 2 better than the aluminum doped cells. K values obtained from the data shown in Figure 19 are presented in Table 2. As shown in Table 2, the K values indicate that the lot one aluminum doped and lot two boron doped 1 ohm-cm cells are similar and superior to the lot one boron doped and lot two aluminum doped cells. There does not appear, therefore, to be any significant difference between the aluminum doped and the boron doped cells. The actual K values obtained are in good agreement with data previously obtained and reported by ourselves[22] and RCA[17]. It is pointed out that the diffusion length data indicates a straight line degradation characteristic as expected with slopes exhibiting a good fit to a minus 0.5 although significant deviation from this slope did appear to occur in the case of the second lot 1 ohm-cm aluminum doped cells.

Short circuit current degradation of the 10 ohm-cm cells is summarized in Figure 20. The second lot aluminum doped 10 ohm-cm cells were the most superior as was the case in the previously described 1 ohm-cm aluminum doped case. On the other hand, examination of the first lot data indicates that in terms of short circuit current degradation, the boron doped cells of the first lot were actually superior to the aluminum doped cells. Examination of the diffusion length degradation characteristics shown in Figure 21 indicate that only the second lot boron doped 10 ohm-cm cells were different than and slightly inferior to the remaining other three types tested. As shown in Table 2, the 10 ohm-cm boron doped cells

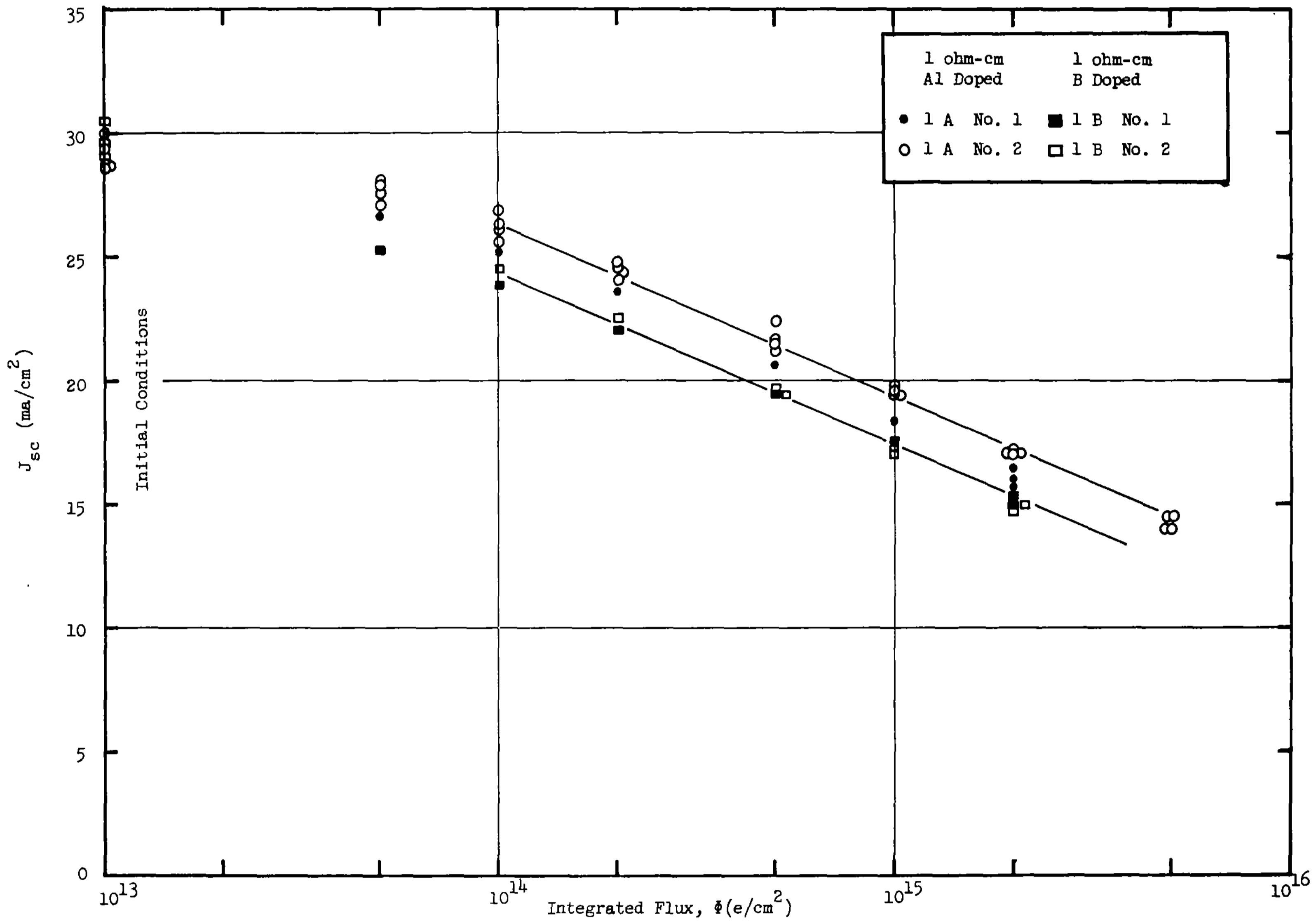

Figure 18. Short Circuit Current Degradation of 1 ohm-cm Silicon Solar Cells Under Electron Irradiation

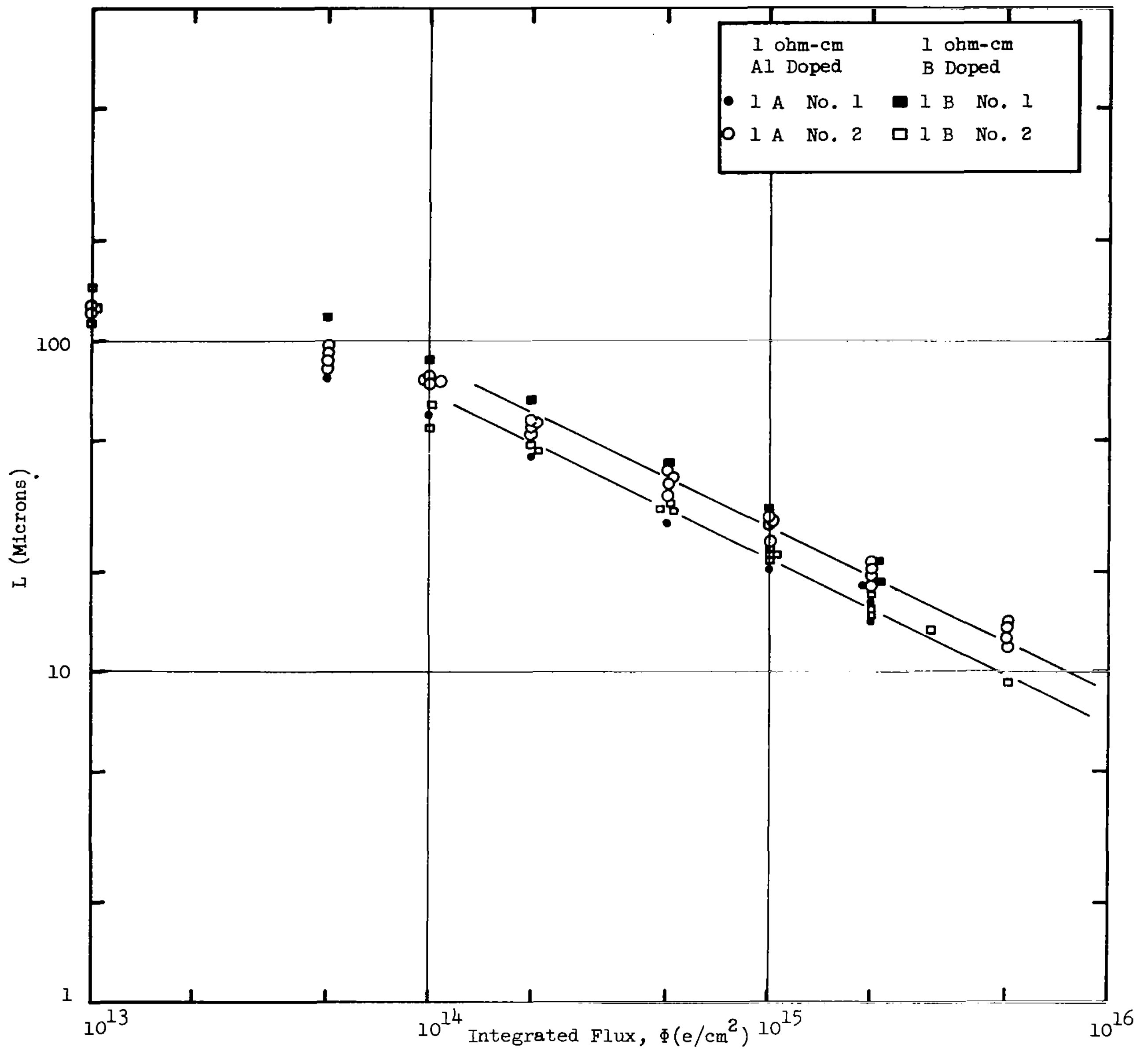

Figure 19. Minority Carrier Diffusion Length Degradation of 1 ohm-cm Silicon Under Electron Irradiation

TABLE II

K Values for Aluminum and Boron Doped Silicon

	1 ohm-cm Aluminum doped	1 ohm-cm Boron doped	10 ohm-cm Aluminum doped	10 ohm-cm Boron doped
Lot 1	$1.7 - 2.5 \times 10^{-10}$	$1.0 - 1.4 \times 10^{-10}$	$5.7 - 6.9 \times 10^{-11}$	$4.7 - 5.2 \times 10^{-11}$
Lot 2	$1.2 - 1.6 \times 10^{-10}$	$1.8 - 2.3 \times 10^{-10}$	$4.7 - 6.3 \times 10^{-11}$	$8.2 - 10 \times 10^{-11}$
STL[22]	-----	$1.5 - 2.5 \times 10^{-10}$	-----	$7 - 9 \times 10^{-11}$
RCA[17]	-----	$1.2 - 1.7 \times 10^{-10}$	$8 - 9 \times 10^{-11}$	$7 - 10 \times 10^{-11}$

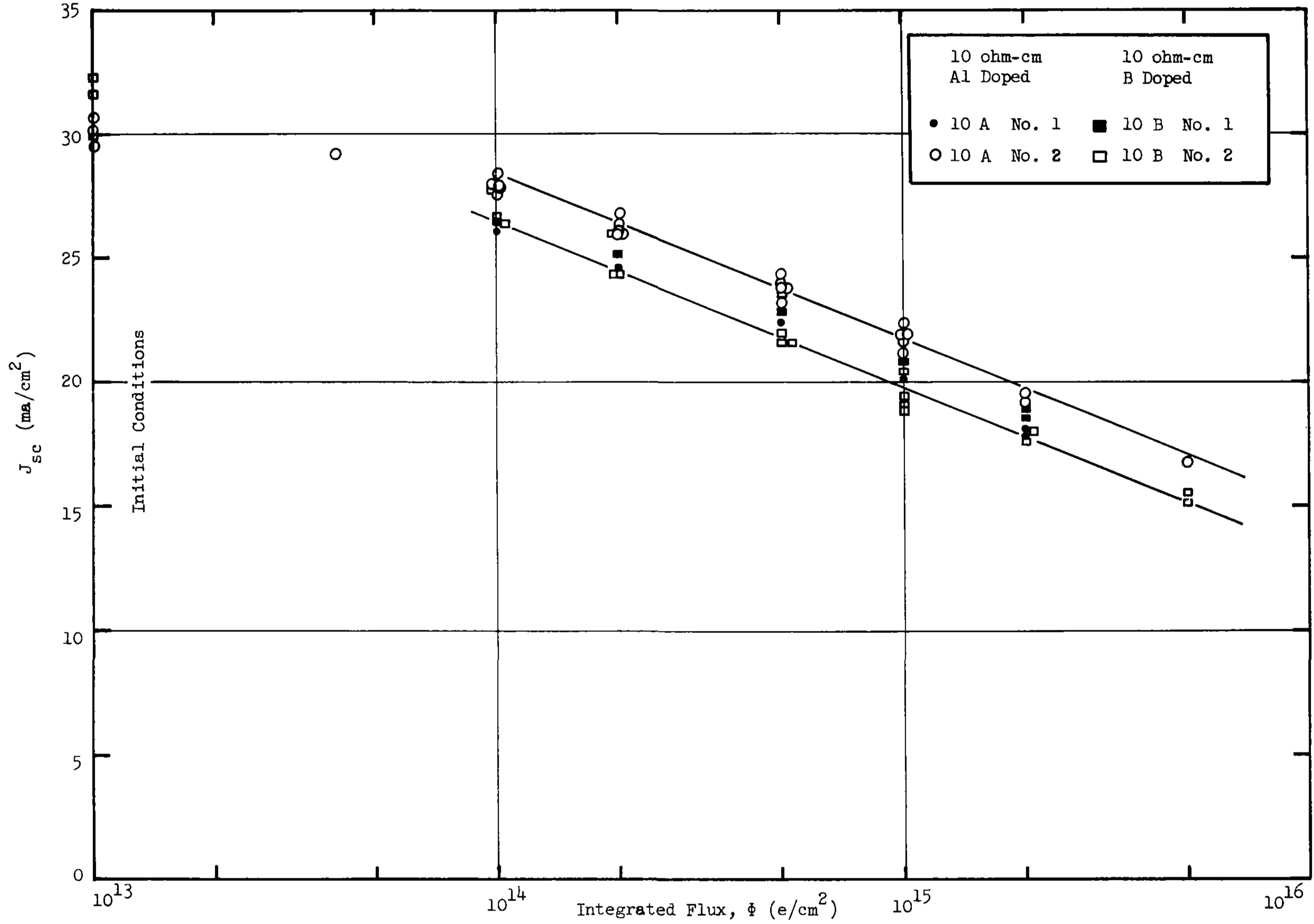

Figure 20. Short Circuit Current Degradation of 10 ohm-cm Silicon Solar Cells Under Electron Irradiation

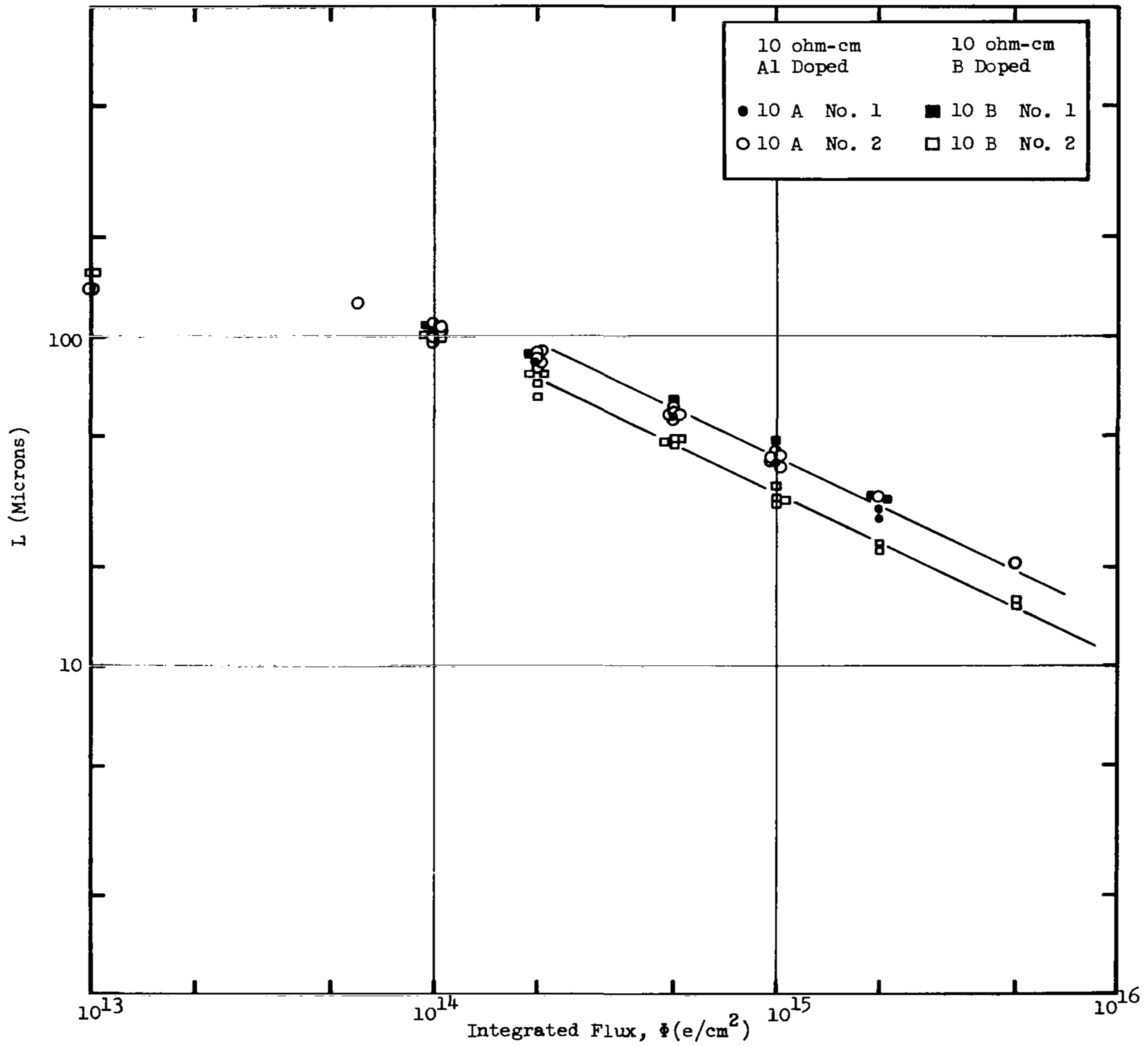

Figure 21. Minority Carrier Diffusion Length Degradation of 10 ohm-cm Silicon Under Electron Irradiation

of the second lot exhibited K values similar to those previously reported; whereas both aluminum doped lots and the boron doped cells of lot number one were superior by almost a factor of 2. As in the case of the 1 ohm cm cells there is no significant difference in K values which can be attributed to a dependence on dopant.

C. Conclusions

A total of 40 n on p silicon solar cells of 1 and 10 ohm-cm boron and aluminum doped base material were irradiated with 1 Mev electrons. Comparison of K values indicates that there is no significant difference in the radiation sensitivity between aluminum doped silicon and boron doped silicon. The only significant difference observed was the expected decrease in sensitivity of the 10 ohm-cm cells relative to the 1 ohm-cm cells. Significant variations were observed as a function of lot number indicating that minor differences in radiation sensitivity in otherwise alike test specimens are introduced in the manufacture of the devices due to either slight differences in fabrication techniques or differences in the actual trace impurity concentrations of the material used for the specimens.

V. SUMMARY

The results of the energy level studies reported in Section II indicate that the electron energy dependence of n on p solar cell damage is similar to that found for the production of the Ev + 0.3 ev energy level. Although the data suggests a relationship, it is not conclusive. The positive identification of the recombination centers for electron damaged solar cells requires a definitive experiment which yields direct information about the controlling defects. As previously mentioned, many attempts have been made to solve this problem. The suggested solutions are not consistent with each other or other known facts. It remains for a consistent analysis of recombination centers in electron irradiated silicon to be made. Theoretical models for this analysis are available. The problems are largely experimental. The minority carrier lifetimes involved impose difficult electronic problems in measurement. There are many approaches and variations for this type of experiment; however, the proposed defect models must explain the known degradation patterns in solar cells. There are two aspects of basic problem. The first is to identify the recombination centers. This includes the determination of the various Hall, Shockley-Read parameters. The second phase of the problem is to determine the physical nature of the recombination centers. Work to identify the centers is limited to investigation of minority carrier lifetime or diffusion length as functions of temperature or majority carrier concentration. The experimental problems involved in such investigations must be solved in such a way to yield reproducable results which can be confirmed by an independent method. After the recombination center is identified, techniques such as Hall coefficient, ESR, infrared absorption, and photoconductivity may be used to determine nature of the defect.

The data presented in Section III clearly illustrate the extreme sensitivity of silicon solar cells to low energy protons. Although the data may suffer shortcomings in the quantitative details of absolute sensitivities due to the compromised proton being used in these experiments, the data qualitatively proves that, at low proton energies, the degradation rates all increase sharply over those observed for more penetrating radiation.

There appears to be a distinct peak in the sensitivity versus energy relationship which lies somewhere between 2 and 6 Mev. Inasmuch as the experiments reported here covered only energies from 0.2 Mev to 1.9 Mev, comparison of these data with previous experiments reported earlier at proton energies down to 6.7 Mev indicate that this peak sensitivity in absolute power output degradation must lie somewhere between 2 and 6 Mev and most probably close to 2 Mev. Based on this information, then, it is evident that further data on low energy proton degradation in the energy region from about 2 Mev to 6 Mev is needed to complete the picture concerning the proton energy dependence of silicon solar cell degradation.

In Section IV, the results of an experiment to determine the effect of aluminum versus boron dopant on the radiation sensitivity of p-type silicon to 1 Mev electron radiation was presented. Analysis of the data based on K values indicates that aluminum and boron doped p-type silicon do not exhibit any marked differences in their radiation sensitivities. Since over 40 different specimens of 4 distinctly different combinations of resistivity and dopant material were tested, the results can be considered statistically significant. It was also observed that wider variances in radiation sensitivity occurred between supposedly alike specimens fabricated at different times than differences observed that could be attributed to variation of dopant material. It is not clear at this writing which direction future efforts on the effect of impurities in silicon should take. Others in the field are currently conducting similar programs with a wide range of dopant materials. Hopefully, when these programs are completed and reported, an analysis of all the current data to date will indicate a reasonable and logical approach to the continuation of efforts in this particular area.

REFERENCES

1. G. K. Wertheim, Physical Review, 105, 1730 (1957).
2. G. K. Wertheim, Physical Review, 110, 1272 (1958).
3. G. N. Galkin, N. S. Rytova and V. S. Vavilov, Soviet Physics - Solid State, 2, 1819 (1961).
4. J. A. Baicker, Physical Review, 129, 1174 (1963).
5. G. Bemski and W. M. Augustyniak, Physical Review, 108, 645 (1957).
6. J. W. Corbett, G. D. Watkins, R. M. Chrenko and R. S. McDonald, Physical Review, 121, 1015 (1961).
7. R. G. Downing, J. R. Carter, and J. M. Denney, Proceedings of the Fourth Photovoltaic Specialists Conference, 1, A-5-1 (1964).
8. D. E. Hill, Physical Review, 114, 1414 (1959).
9. G. D. Watkins and J. W. Corbett, Physical Review, 121, 1001 (1961).
10. G. D. Watkins and J. W. Corbett, Physical Review, 134, A1359 (1964).
11. G. Bemski, B. Szymanski, and K. Wright, Journal of Chemistry and Physics of Solids, 24, 1 (1963).
12. H. Saito, M. Hirata, and T. Horiuchi, Journal of the Physical Society of Japan, 18 III, 246 (1963).
13. J. R. Carter, Jr., IEEE Trans. NS-11, 290 (1964).
14. G. W. Ludwig and R. L. Watters, Physical Review, 101, 1699 (1956).
15. F. Seitz and J. W. Koehler, "Displacement of Atoms During Irradiation," Solid State Physics, Vol. 2, Academic Press, New York (1956).
16. G. D. Watkins and J. W. Corbett, Physical Review, 138, A543 (1965).

    J. W. Corbett and G. D. Watkins, Physical Review, 138, A555 (1965).
17. Radio Corporation of America, Final Report, "Radiation Damage in Silicon," Contract NAS5-3788, December 1964.
18. P. H. Fang, Personal Communication.
19. J. M. Denney, et al, "Charged Particle Radiation Damage in Semiconductors, IV: High Energy Proton Radiation Damage in Solar Cells," Report No. 8653-6017-KU-000, Contract NAS5-1851, (20 January 1963), TRW Space Technology Laboratories, Redondo Beach, Calif.
20. J. M. Denney and R. G. Downing, "Charged Particle Radiation Damage in Semiconductors, I: Experimental Proton Irradiation of Solar Cells," Report No. 8987-0001-RU-000, Contract NAS5-613, (15 September 1961), TRW Space Technology Laboratories, Redondo Beach, Calif.

REFERENCES (Con't)

21. J. Mandelkorn, Proceedings of the Fourth Photovoltaic Specialists Conference, 1, A-6-1 (1964).

22. J. M. Denney, et al, "Charged Particle Radiation Damage in Semiconductors, V: Effect of 1 Mev Electron Bombardment on Solar Cells," Report No. 8653-6018-KU-000, Contract NAS5-1851, (11 February 1963), TRW Space Technology Laboratories, Redondo Beach, Calif.

NASA-Langley, 1966 CR-404